atmosphere

MDPI

Article

Interannual Variability and Trends in Sea Surface Temperature, Lower and Middle Atmosphere Temperature at Different Latitudes for 1980–2019

Andrew R. Jakovlev [1], Sergei P. Smyshlyaev [1,*] and Vener Y. Galin [2]

[1] Department of Meteorological Forecasting Voronezhskaya, Russian State Hydrometeorological University, Str., 79, 192007 Saint-Petersburg, Russia; endrusj@rambler.ru
[2] Institute of Numerical Mathematics RAS, Gubkina Str., 8, 119991 Moscow, Russia; venergalin@yandex.ru
* Correspondence: smyshl@rshu.ru

Abstract: The influence of sea-surface temperature (SST) on the lower troposphere and lower stratosphere temperature in the tropical, middle, and polar latitudes is studied for 1980–2019 based on the MERRA2, ERA5, and Met Office reanalysis data, and numerical modeling with a chemistry-climate model (CCM) of the lower and middle atmosphere. The variability of SST is analyzed according to Met Office and ERA5 data, while the variability of atmospheric temperature is investigated according to MERRA2 and ERA5 data. Analysis of sea surface temperature trends based on reanalysis data revealed that a significant positive SST trend of about 0.1 degrees per decade is observed over the globe. In the middle latitudes of the Northern Hemisphere, the trend (about 0.2 degrees per decade) is 2 times higher than the global average, and 5 times higher than in the Southern Hemisphere (about 0.04 degrees per decade). At polar latitudes, opposite SST trends are observed in the Arctic (positive) and Antarctic (negative). The impact of the El Niño Southern Oscillation phenomenon on the temperature of the lower and middle atmosphere in the middle and polar latitudes of the Northern and Southern Hemispheres is discussed. To assess the relative influence of SST, CO_2, and other greenhouse gases' variability on the temperature of the lower troposphere and lower stratosphere, numerical calculations with a CCM were performed for several scenarios of accounting for the SST and carbon dioxide variability. The results of numerical experiments with a CCM demonstrated that the influence of SST prevails in the troposphere, while for the stratosphere, an increase in the CO_2 content plays the most important role.

Keywords: reanalysis data; chemistry-climate model; southern oscillation; El-Nino; La-Nina; sea surface temperature; temperature of air; CO_2; low troposphere; low stratosphere

Citation: Jakovlev, A.R.; Smyshlyaev, S.P.; Galin, V.Y. Interannual Variability and Trends in Sea Surface Temperature, Lower and Middle Atmosphere Temperature at Different Latitudes for 1980–2019. *Atmosphere* **2021**, *12*, 454. https://doi.org/10.3390/atmos12040454

Academic Editors: António Tomé and Eugene Rozanov

Received: 3 March 2021
Accepted: 23 March 2021
Published: 2 April 2021

1. Introduction

Weather and climatic processes are largely determined by the interaction of the atmosphere and the ocean. In particular, simultaneous long-term changes in the temperature of the sea surface and the atmosphere can influence each other, changing the radiation regime and the dynamics of the atmosphere and the sea. In addition to long-term variability on a scale of several decades, short-term changes in sea surface temperature on a scale of several years can also affect atmospheric parameters. One of the most well-known short-term changes affecting both marine and atmospheric characteristics is the El Niño—Southern Oscillation (ENSO), which has El Niño and La Niño phases. Warming of the sea surface (El Niño phase) as well as cooling of the sea surface (La Niño phase) in the equatorial Pacific Ocean not only affects regional weather and climate changes, but also controls the general circulation of the atmosphere, which determines changes in air temperature and trace atmospheric gases at different altitudes in extratropical latitudes [1,2].

The atmospheric component of El Niño is the Southern Oscillation [1–3], in which there are fluctuations in atmospheric pressure between the eastern and western Pacific.

Due to the low pressure in the eastern part, deep convection begins. Warm water increases evaporation and humidity in western South and Central America, resulting in heavy rains, thunderstorms, floods, and hurricanes. It also weakens the trade winds, leading to drought in Australia. At the same time, an increase in vertical flows of heat, mass, and momentum also affects their horizontal transport, disturbing the general circulation of the atmosphere and creating the potential for changes in temperature and gas composition in other regions, not only in the troposphere, but also in the stratosphere [3].

La Niña is the cold phase of ENSO, during which the temperature of the upper ocean layer drops [1,2]. At the same time, atmospheric pressure rises and convective processes weaken. The interaction of the ocean and the atmosphere, including ENSO phenomenon, is a topical subject of various scientific studies, thanks to which various models have been developed to analyze and predict this phenomenon. Currently, there are a huge variety of such models. These models make it possible to analyze the temperature anomalies of the sea surface simultaneously with the processes occurring in the atmosphere, which, in turn, makes it possible to study the relationship between them [4,5]. Using such models, the influence of ENSO on weather and climate in South America and Australia was investigated [4–6]. At the same time, it has recently become especially urgent to study the influence of the ocean [6] and ENSO on global processes occurring in the earth system, with special attention to their impact on the stratosphere and processes in the polar regions [7–9].

The meridional sea-surface temperature (SST) gradient, changing as a result of periodic changes in sea surface temperature (SST), can have a significant impact on the stratosphere [10]. The meridional SST gradient has a stronger effect on the zonal circulation than the global SST variability. One of the significant effects of the variability of the SST meridional gradient is its effect on the stability of the polar vortex and the ozone content in the Northern Hemisphere. Modeling reveals that, in general, the influence of El Niño on the parameters of the Earth's climate occurs through stratospheric processes [11]. On the other hand, some studies suggest that a decrease in the content of stratospheric ozone in the tropics may trigger the El Niño phase of the Southern Oscillation, and an increase in its content may lead to the La Niña phase [12]. This can happen as a result of changes in ocean heating by solar radiation passing through the ozone layer.

Long-term and short-term changes in sea surface temperature, affecting the general circulation of the atmosphere and its wave activity, can impact the stability of the polar vortex and the temperature of the polar stratosphere. The temperature of the lower polar stratosphere, which determines the appearance and development of the polar stratospheric clouds, is an important factor in the winter-spring decrease in ozone content. The cold winter seasons of 1996–1997, 2010–2011, 2015–2016, and 2019–2020 led to an increase in ozone loss in a stable polar vortex with weakened activity of atmospheric planetary waves. In general, warm winter seasons in the polar regions are usually characterized by an increase in wave activity at the edge of the polar vortex [13]. The increased and decreased activity of atmospheric planetary waves can be a consequence of the variability of the sea surface temperature, including in the equatorial zone. In turn, the weakening of planetary waves can lead to a decrease in polar temperature and a weakening of ozone transport, which can lead to heating of the tropical tropopause [14,15].

Along with the ocean, changes in the atmospheric temperature are significantly influenced by changes in the content of greenhouse gases and, first of all, carbon dioxide CO_2, which affect the delay of outgoing radiation from the Earth's surface, which leads to an increase in the average air temperature at the surface [16–18]. In addition, as shown by studies using the NCAR community climate system model, version 3.5 (CCSM3.5), changes in CO_2 can also affect the ENSO events [19].

Understanding how ENSO will change in the future climate is of great importance [20–22]. An attempt to estimate the influence of ENSO was made in the general circulation models (GCMs) of the atmosphere [23–25]; however, the influence of CO_2 directly on ENSO was not taken into account. Registration of ENSO events during monitoring of the Pacific Ocean, starting in 1980, led to the creation of the Tropical Atmosphere Ocean (TAO)

database [26]. The acquisition of SST data has been going on since the 19th century [27,28]. Due to the limitations associated with the ENSO observational data, it was difficult to determine the conditions for their occurrence [29,30]. By means of modeling with the Geophysical Fluid Dynamics Laboratory Climate Model version 2.1 (GFDL CM2.1), the amplitude corresponding to ENSO was determined [31]. However, many models did not betray the significance of the effect of CO_2 on the ENSO amplitude. Studies using Coupled Model Intercomparison Project phase 5 (CMIP5) analysis also did not show a significant relationship [32]. Therefore, this interaction is based on the physics of equilibrium changes in ENSO due to an increase in CO_2, in the absence of transient effects [19].

Studies of temperature trends at different heights of the atmosphere are a topical subject of many recent scientific studies [33–36]. Studying the features of these trends is an important component of climate monitoring [37,38]. Trends in tropospheric warming and stratospheric cooling during the 20–21 centuries were studied on the basis of measurements of radiosondes and microwave sounding of the atmosphere [37,39,40]. The results of sounding and satellite observations were analyzed using climate models [41–43]. Simultaneous stratospheric temperature trends and changes in chemical processes were studied by comparing satellite observations and chemistry-climate modeling [34,44,45]. In a number of works, special attention was paid to the study of the features of warming in the tropics [46,47].

Studies of the vertical features of temperature trends revealed warming of the troposphere and cooling of the stratosphere [48–50]. In [34], the cooling of the stratosphere and its increase with height was associated with an increase in the concentration of greenhouse gases. It was found that the main factor of cooling in the lower stratosphere is a decrease in the ozone content, while the main role in the middle stratosphere is played by an increase in the content of greenhouse gases [33,34]. Quantitative estimates reveal a decrease in stratospheric temperature by 1–3 K over the past 40 years [33]. In this case, the lower stratosphere is cooled by -0.25 K per decade, while the average stratosphere is up to -0.5 K per decade [33]. At the same time, the cooling of the stratosphere is more significant in the Northern Hemisphere than in the Southern Hemisphere [33].

The results of chemistry-climate modeling of tropospheric and stratospheric temperature variability based on the given scenarios of changes in the atmospheric content of greenhouse gases and ozone-depleting substances (ODS), as well as taking into account other factors, such as volcanic aerosol and solar activity, are generally in good quantitative agreement with satellite measurements [43]. These results help to clarify many of the problems in understanding recent trends in tropospheric and stratospheric temperature. Nevertheless, some issues of tropospheric and stratospheric temperature variability, in particular latitudinal features of trends, are still not fully understood [34].

In this work, simultaneous trends and short-term variability of the sea surface and atmospheric temperature are estimated for the different regions and altitudes based on the reanalysis data and numerical experiments with a global chemistry-climate model for the last forty years (1980–2019). Special attention is paid to comparing the effect of sea surface temperature variability and greenhouse gases on tropospheric and stratospheric temperature changes based on calculations with the chemistry-climate model (CCM) for several scenarios of accounting for these factors. This work is a continuation of previous works for a shorter period of time [51–54]. Section 2 describes the methodology, data, and chemistry-climate model used. The results of assessing trends and short-term variability in sea surface and atmospheric temperature at different heights are presented in Section 3. Section 4 presents the results of numerical experiments with a global chemistry-climate model, in which the relative influence of sea-surface temperature variability and greenhouse gas content on tropospheric and stratospheric temperatures at different latitudes is estimated. Section 5 contains discussion and Section 6 is conclusion.

2. Methodology, Data and Model Description

The reanalysis MERRA2 [55], ERA5 [56] and Met Office [57] data were used to study the interannual variability of the sea surface temperature (SST) and the temperature of the lower troposphere and lower stratosphere. Sea surface temperature variability is analyzed using Met Office and ERA5 data, while atmospheric temperature variability is analyzed using MERRA2 and ERA5 data. The reanalysis data were interpolated into the Institute of Numerical Mathematics of the Russian Academy of Sciences (INM RAS)—Russian State Hydrometeorological University (RSHU) chemistry-climate model [58] grid (72 grids in longitude from −185 to 175 degrees with a step of 5 degrees, 45 grids in latitude from −88 to 88 degrees with a step of 4 degrees, 31 pressure levels from the surface to the mesopause with a variable step). The reanalysis data were averaged for each month, as well as for each year from 1980 to 2019.

Produced by the European Centre for Medium-Range Weather Forecasts (*ECMWF*) ERA Interim is a global atmospheric reanalysis that is available from 1 January 1980 to 31 December 2019 [56]. It provides hourly estimates of a large number of atmospheric, land, and oceanic climate variables. The data assimilation system used to produce ERA5 includes a 4-dimensional variational analysis (4D-Var) with a 12-h analysis window. The spatial resolution of the dataset is approximately 80 km (T255 spectral) on 60 levels in the vertical from the surface up to 0.1 hPa. ERA Interim has been superseded by the ERA5 reanalysis, which covers the Earth on a 30 km grid and resolve the atmosphere using 137 levels from the surface up to a height of 80 km [56]. Produced by the National Aeronautics and Space Administration (NASA) the Modern-Era Retrospective analysis for Research and Applications, Version 2 (MERRA2) provides atmospheric data from 1980 up to today [55]. It uses GEOS model with an assimilation system to produce long-term global reanalysis based on ground and space-based observations. Produced by the Met Office Hadley Centre, sea ice and sea surface temperature datasets are based on NOAA and METOP observations. Met Office sea surface temperatures are reconstructed using a two stage reduced-space optimal interpolation procedure, followed by superposition of quality-improved gridded observations onto the reconstructions to restore local detail [57].

To calculate trends in SST and atmospheric parameters, a linear regression equation and multiple regression analysis following [33], with an estimate of the trend significance, were used. The multivariate regression model includes a linear trend term and terms accounting solar cycle, ENSO, and stratospheric aerosol loading. Solar variability was presented by year mean sunspot number [59], ENSO by Met Office SST at tropical part of Pacific Ocean, and stratospheric aerosol by particle surface area [60]. For the analysis, the calculated linear trend coefficient (degrees per decade for sea surface and atmospheric temperatures) was used. For all calculated trends, their statistical significance was estimated by Fisher's criterion [61] by comparing the coefficient of the linear trend with the spread of data relative to the regression line. The probability density function (PDF) and coefficient of determination (R^2) were evaluated. In order to estimate linear regression significance, Fisher's criterion analysis of variance (ANOVA) was used for the sum of squares (SS). For estimation of the probability density function (PDF) that regression is significant, the cutoff value $F = (N-2)SS_E/SS_R$, where N is number of points, SS_R—sum of squares for regression, and SS_E—sum of squares for residuals, with N-2 degrees of freedom, is used to calculate probability for F distribution [61]. The significance level for calculated F-value is assessed as difference between 1 and PDF. The coefficient of determination, which provides the part of total variance explained by the regression, is estimated as $R^2 = 1 - SS_R/SS_{Tot}$. Trends and short-term variability were analyzed for the lower troposphere (pressure levels from 1000 to 600 mb) and the lower stratosphere (pressure levels from 200 to 30 mb) of tropical, middle, polar latitudes, and on average over the globe.

To assess the role of SST and CO_2 affecting the interannual variability of the lower troposphere and low stratosphere temperature, numerical experiments with the INM RAS–RSHU CCM [58,62,63] were performed. The model has a spatial resolution of 4 × 5 degrees latitude/longitude and covers the altitude range from the Earth's surface up to the

mesopause (around 90 km) with 39 sigma-pressure levels with variable pressure spacing [58,62,63]. In order to take into account an interaction between chemical and dynamical processes in the low and middle atmosphere under the frame of a CCM, a INM RAS General Circulation Model (GCM) is interactively coupled with a RSHU global chemistry-transport model (CTM), which was designed based on the three-dimensional extension of the SUNY-SPB two-dimensional model [58,62,63]. In addition to temperature and dynamical variables, the CCM calculates variability of 74 chemically active gases in the lower and middle atmospheres, which are interacting in 174 gas-phase and heterogeneous chemical reactions and 51 photodissociation processes, including oxygen, nitrogen, hydrogen, chlorine, bromine, carbon, and sulfur cycles [58,64], and takes into account gas concentrations impact on the temperature. The model considers the processes of the formation and evolution of polar stratospheric clouds (PSC) based on the stratospheric sulfate aerosol distribution [58]. Polar vortex dynamics are resolved by the CCM based on dynamical core of INM RAS GCM [58,64].

The influence of sea surface temperature on atmospheric characteristics in INM RAS—RSHU CCM is taken into account by setting a lower boundary condition in the air temperature evolution equation. For those CCM grids that have sea surface at low boundary, the temperature at the lower boundary is set by temporal interpolation of the SST monthly average reanalysis data. In addition, the area of ice coverage of the sea is also taken into account, which is also determined from the reanalysis data. To assess the influence of SST variability on the interannual variability of atmospheric characteristics in the background of an increase in the content of greenhouse gases in the atmosphere, calculations using the CCM were performed for the period 1979–2019 according to several scenarios. In the first (BASE) scenario, the variability of both SST and carbon dioxide content was taken into account, in the second (CO2FIX), atmospheric carbon dioxide content was fixed at the 1979 level, in the third (SSTFIX), SST was fixed at the 1979 level, taking into account seasonal variability, and finally, in the fourth scenario (FIX), the values of carbon dioxide and SST were fixed at the 1979 level. In all four scenarios, interannual variability of greenhouse gases (Climate System Scenario Tables [65]) and ozone-depleting substances (data of WMO-2018 [66]) was set. Results of model estimation were interpolated to the 31 vertical pressure levels (14 levels in the troposphere and 17 levels in the stratosphere and mesosphere).

3. Simultaneous Change of Sea Surface and Air Temperature Trend and Short-Term Variability Based on Reanalysis Data

Figure 1 presents the variability of the sea surface temperature (SST) averaged over the entire globe (upper plot) and for the tropics (lower plot) according to the reanalyzes of Met Office and ERA5. According to all data, during the period from 1980 to 2019, both in the tropics and across the globe, there is a significant (1% significance level) positive SST trend. In the tropics, both datasets show similar trends of about 0.1 degrees per decade. At the same time, a slightly larger trend is obtained according to ERA5 data. A significant short-term increase in SST can be noted in 1982–1983, 1986–1987, 1997–1998, 2009–2010, and 2014–2016 for variability with a period of several years in the tropical zone, corresponding to the El Niño phase of the Southern Oscillation and decreased SST values 1984–1985, 1989–1990, 1996, 1999–2000, 2008, and 2010–2011, corresponding to the La Niña phase of the Southern Oscillation. In accordance with the coefficient of determination, about half of the SST variance in the tropics is explained by a linear trend, and the second half is described by short-term variability.

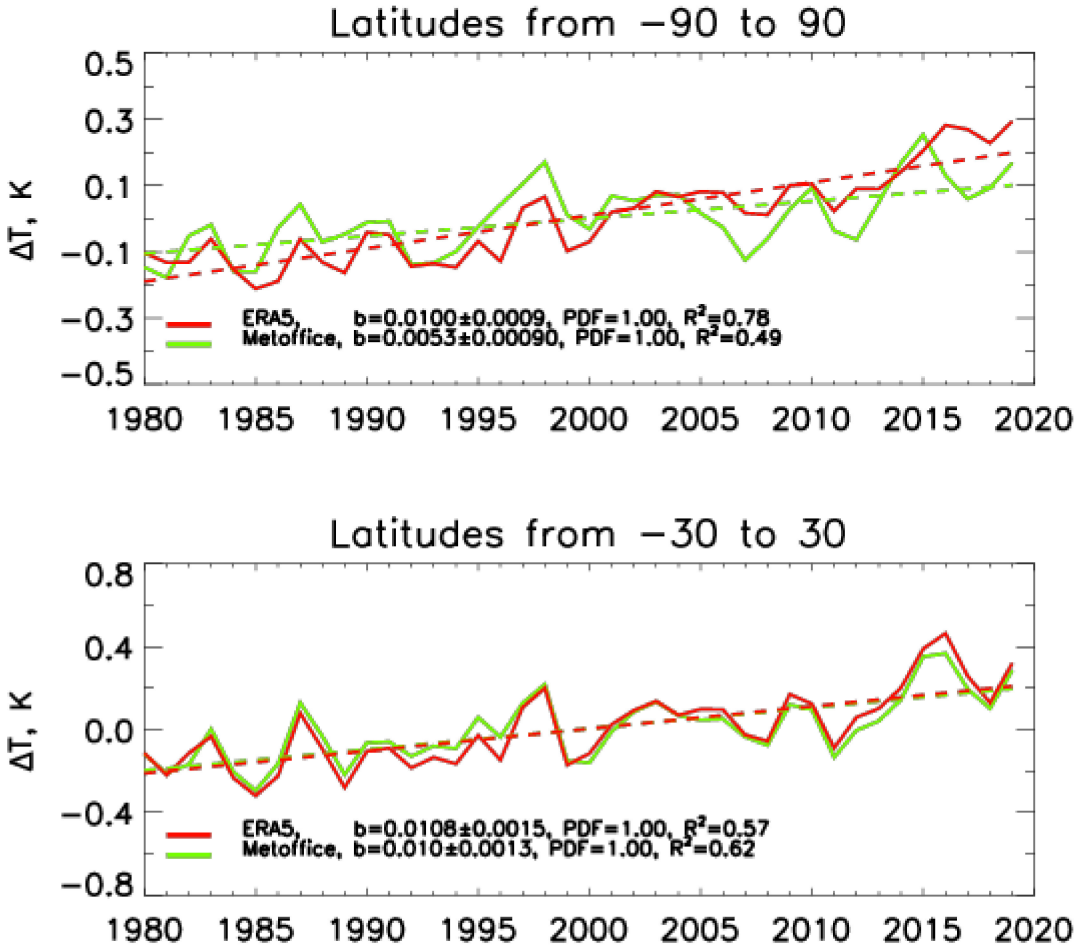

Figure 1. Interannual variability of sea surface temperature anomalies: globally (**top**) and for the tropics (**bottom**) with an assessment of trends (degrees per year) and their significance based on the reanalysis data ERA5 (red) and MetOffice (green).

Globally, the estimates of trends differ almost twofold: The ERA5 data reveal a trend of about 0.1 degrees per decade, and the Met Office data reveal that of about 0.05 degrees per decade (Figure 1, top). All trends are significant with a 1% significance level. The short-term variability of the SST is also quite different between different reanalysis datasets. At the same time, for all reanalysis data on a global scale, periods of increase and decrease in SST are repeated corresponding to the most powerful phases of El Niño (1982–1983, 1986–1987, 1997–1998, 2009–2010, and 2014–2016) and La Niño (1984–1985, 1989–1990, 1996, 1999–2000, 2008, and 2010–2011). The largest amplitudes of SST fluctuations on a global scale are shown by the Met Office data, while in some years, the phases of the minima and maxima of Met Office and ERA5 do not coincide. Accordingly, about a half of the global mean SST variance in the Met Office data is described by short-period variability (about 51%), while for the ERA5 data, on the contrary, about 80% of the variance explained by a linear trend. In general, a comparison of the interannual variability of SST on a global scale and in the tropics indicates that the phases of the Southern Oscillation, which have a tropical nature, have a significant impact on SST changes on a global scale.

Figure 2 presents the interannual variability of the SST in the middle latitudes of the Southern (bottom) and Northern (top) Hemispheres. In the Northern Hemisphere, SST trends for the period from 1980 to 2019, according to Met Office and ERA5 data (about 0.2 degrees per decade), are twice as large as in tropical latitudes and globally. In the middle latitudes of the Southern Hemisphere, on the contrary, the SST trend is significantly less than on a global scale and in the tropics. In the Southern Hemisphere, SST trends are 5 times less than in the Northern Hemisphere (0.025–0.035 degrees per decade), which, on the one hand, indicates a significant difference in ocean processes in different

hemispheres, and on the other hand, shows that in addition to the anthropogenic factor of global warming, which potentially should have the same effect in different hemispheres, the natural variability, which is different in different hemispheres, probably plays an important role, and, thirdly, creates the potential for different effects of SST variability on atmospheric parameters in different hemispheres. The short-term variability of SST at mid-latitudes has a rather pronounced seasonal variability, which veils interannual fluctuations. Nevertheless, against the background of seasonal variability, the influence of the Southern Oscillation is noticeable in some years. An analysis of the coefficients of determination detects that, despite the fact that SST trends are significant in both hemispheres with a 1% significance level, in the Northern Hemisphere, the trend describes more than 80% of the variance, and in the Southern Hemisphere, it explains only 17% for the ERA5 data and 55% for the Met Office data.

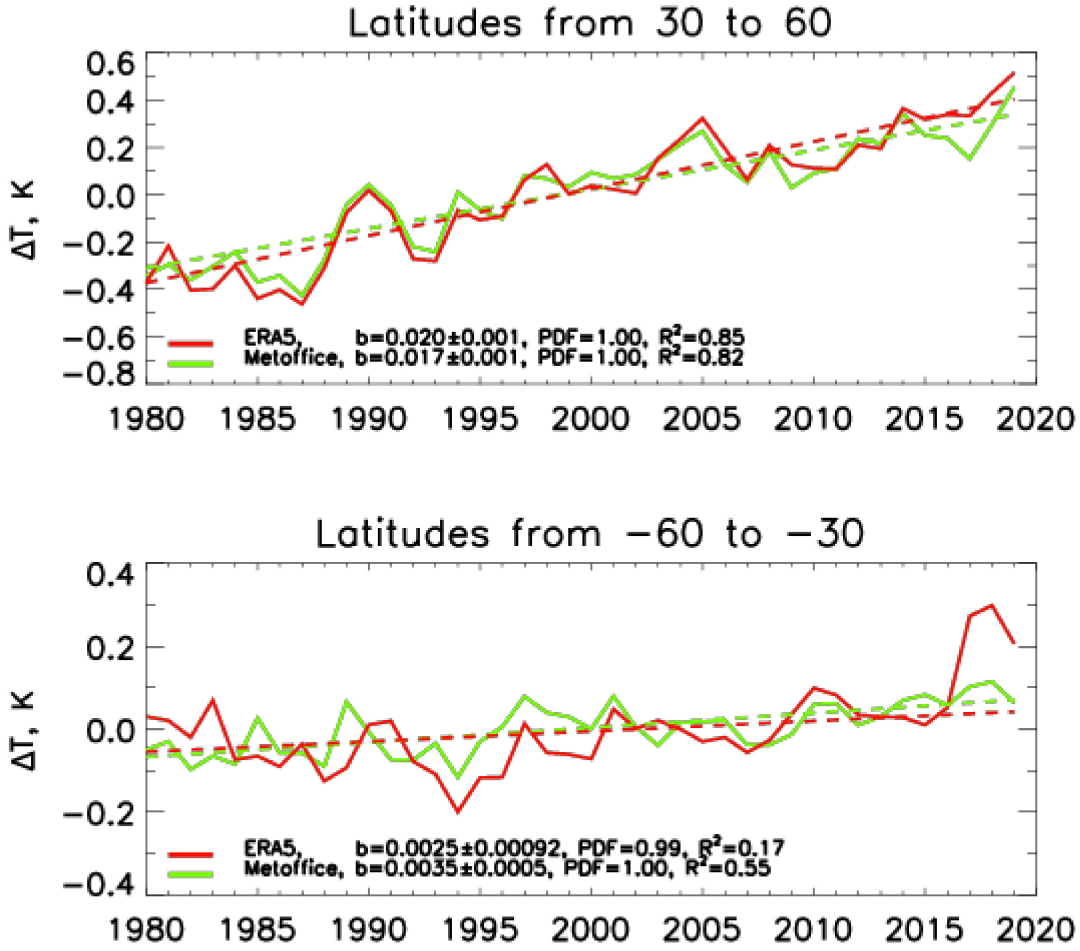

Figure 2. Interannual variability of sea surface temperature anomalies for the middle latitudes of the Northern Hemisphere (**top**) and Southern Hemisphere (**bottom**) with an estimate of trends (degrees per year) and their significance based on the reanalysis data ERA5 (red) and MetOffice (green).

Figure 3 presents the interannual SST variability in the polar regions of the Southern (bottom) and Northern (top) Hemispheres. The data of both reanalysis data demonstrate differently directed significant (1% significance level) trends. In the polar latitudes of the Northern Hemisphere, the reanalysis data give a positive trend: ERA5, about 0.13 degrees per decade, and Met Office, about 0.04 degrees per decade, while in the Southern Hemisphere, according to reanalysis data, a negative SST trend is obtained: ERA5 is about −0.06 degrees per decade, and Met Office is about −0.02 degrees per decade. Negative SST trend near Antarctic may be caused by an increased wind-driven northward sea-ice

transport, enhancing the extraction of freshwater near Antarctica and releasing it in the open ocean [67].

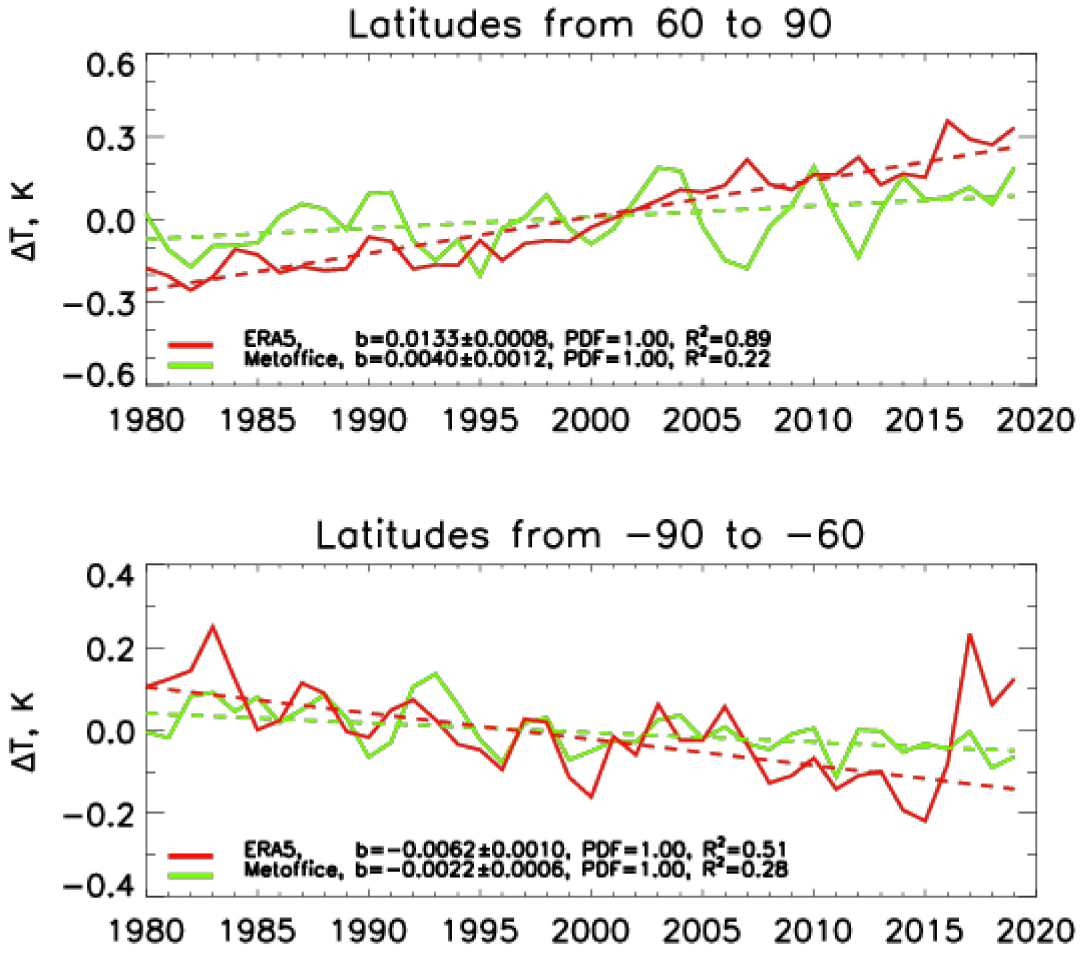

Figure 3. Interannual variability of sea surface temperature anomalies for the polar latitudes of the Northern Hemisphere (**top**) and Southern Hemisphere (**bottom**) with an estimate of trends and their significance based on the reanalysis data ERA5 (red) and Met Office (green).

At the same time, after 2016, ERA5 data demonstrate a significant increase in SST in the polar zone of the Southern Hemisphere. The short-term variability in the polar regions demonstrates a decrease in the minimum SST in the Southern Hemisphere and an increase in the maximum SST in the Northern Hemisphere. This can affect dynamic conditions affecting atmospheric parameters in the lower and middle atmosphere.

The polar regions are characterized by large differences between ERA5 and Met Office data. Trends according to Met Office have low values in both the Northern and Southern Hemispheres, although they are significant at a 1% significance level, but with a low coefficient of determination. At the same time, short-term variability explains more than 80% of the variance in the Northern Hemisphere and more than 70% of the variance in the Southern Hemisphere. At the same time, the trend estimated from the ERA5 data describes almost 90% of the variance in the Northern Hemisphere, but about a half in the Southern Hemisphere. Wherein, similar to middle latitudes, the ERA5 data have a strong increase in SST in the Southern Hemisphere after 2016, which increases the contribution of short-term variability to the total variance.

Figure 4 shows the SST variability in the Southern Oscillation region (equatorial part of the Pacific Ocean) according to the Met Office and ERA5 reanalysis data (top) and the change in air temperature in the lower troposphere in the tropics (middle) and globally (bottom) according to the ERA5 and MERRA2 reanalysis data. In the South Oscillation

region, the SST trend is insignificant if one focuses on the 1 or 5% significance level, and the Southern Oscillation phases correspond to the SST maximum (El Niño phase) in 1982–1983, 1986–1987, 1991–1992, 1994–1995, 1997–1998, 2002–2003, 2004–2005, 2007, 2009–2010, and 2014–2016, and the minimum SST (La Niña phase) in 1989, 1996, 2000, 2006,2008, 2011, and 2018 [51,67–69]. Almost all variance is explained by the short-term variability mostly associated with ENSO.

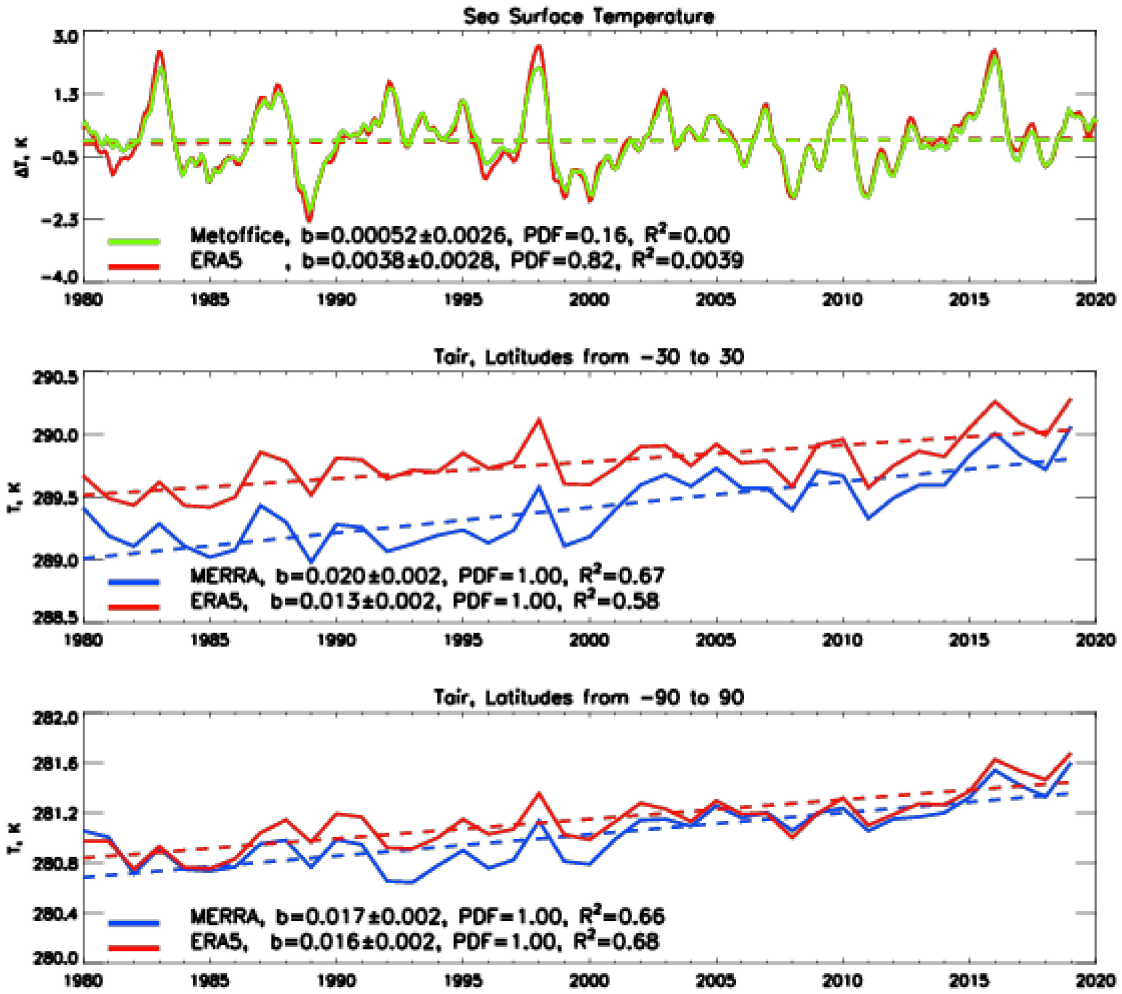

Figure 4. Interannual variability of sea surface temperature anomalies in the Southern Oscillation region based on the reanalysis data ERA5 (red), Met Office (green) (**top**), and air temperature in the lower troposphere for the tropics (**middle**) and globally (**bottom**) based on the reanalysis data MERRA(blue) and ERA5 (red) with an assessment of trends (degrees per year) and their significance.

The change in air temperature in the tropical zone shown in Figure 4 (middle) demonstrates a positive trend, significant at a significance level of 1%, with values of 0.2 degrees per decade for the MERRA2 reanalysis and 0.13 degrees per decade for the ERA5 reanalysis. The short-term variability of air temperature in the lower troposphere of the tropics clearly follows the phases of the Southern Oscillation. It can be noted that the ERA5 data exceed the MERRA2 data by 0.5 degrees in the early 1980s of the XX century and by 0.1 degrees at the end of the 2010s of the XXI century. The difference is decreasing due to the fact that the trend according to MERRA2 data is almost twice as large as according to ERA5.

The global variability of the temperature of the lower troposphere (bottom of Figure 4) is close for the MERRA2 and ERA5 reanalysis data. The trend is about 0.15 degrees per decade, which is slightly less than ERA5 tropical trend and slightly larger than MERRA2 tropical trend, and explains about 65–70% of the total variance. The short-term variability in

the temperature of the lower troposphere on a global scale, as well as in the tropics, follows the SST variability in the ENSO region and describes about 30% of the total variance.

Figure 5 presents the variability of air temperature in the lower troposphere of the middle latitudes of the Northern Hemisphere (top) and the Southern Hemisphere (bottom) according to the MERRA2 and ERA5 reanalysis data. Estimation of trends in surface air temperature shows their positive values of slightly more than 0.2 degrees per decade in the Northern Hemisphere and two times less in the Southern Hemisphere (0.07–0.09 degrees per decade). Trends are significant with a 1% significance level. The values of the air temperature trends in the lower troposphere at middle latitudes are in good agreement with the SST trends in the middle latitudes of the Northern Hemisphere and are twice as large as the SST trends in the middle latitudes of the Southern Hemisphere (Figure 2). The short-term variability of the surface air temperature in the middle latitudes of the Northern Hemisphere also, on the whole, coincides with the short-term variability of the SST in the middle latitudes, with maximums in 1981, 1983, 1990, 1998, 2005, and 2014 and minimums in 1985, 1992–1993, 1996, 2009, and 2011. In the middle latitudes of the Southern Hemisphere, the coincidence of the short-term variability of air temperature and SST is somewhat worse than in the Northern Hemisphere. The coincidence of the maximums of 1990, 2001, 2010, and 2017 can be noted. At the same time, in 1998, when the most powerful El Niño phenomenon was observed, which was reflected in the change in air temperature in the middle latitudes of both hemispheres and the SST of the Northern Hemisphere, a minimum was noted in the SST of the middle latitudes of the Southern Hemisphere (Figure 2). The El Niño events of 1992, 2003, 2008, and 2016 are not reflected in the variability of surface air temperatures in both hemispheres. It should also be noted the systematic difference in the temperatures of the lower troposphere at middle latitudes for the MERRA2 and ERA5 data. The ERA5 reanalysis data exceed the MERRA2 values by 0.5 degrees in the Northern Hemisphere and by 0.2 degrees in the Southern Hemisphere.

The interannual variability of the surface air temperature in the polar regions according to the MERRA2 and ERA5 reanalysis data is shown in Figure 6. In the Arctic region, there are maximum positive temperature trends of about 0.45 degrees per decade, which is more than two times higher than the global average for both air temperature (Figure 4) and SST (Figure 1). The maximum trends in the Arctic correspond to the phenomenon of the Arctic amplification [52,64,65,69]. At the same time, the temperature trend in the Arctic is three times higher than the maximum local SST trend according to ERA5 data and 10 times higher than the minimum SST trend according to Met Office data (Figure 3). The short-term variability of air temperature in the lower troposphere of the Arctic has maximums in 1981, 1984–1985, 1988, 1990, 1995, 1998, 2002–2003, 2005, 2010, 2012, and 2016. Compared to the El Niño phases of the Southern Oscillation, these maximums coincide for the El Niño phases of 1988, 1995, 1998, 2003, 2010, and 2016. As in the middle and tropical latitudes, ERA5 data systematically exceed MERRA2 values by about 0.5 degrees.

In Antarctica, the surface air trend is weakly negative and insignificant for the 5% significance level. More than 99% of the total variance is explained by short-term variability in the Southern polar region, while in the Northern polar region, more than 65% of total variance is described by the trend. The short-term variability of the temperature of the lower troposphere in the Antarctic region has maximums in 1984, 1988, 1991, 1996, 1998, 2002, 2005, 2007, 2011, and 2016. These highs correspond to El Niño events in 1988, 1988, and 2016. Unlike other areas of the globe, in Antarctica, MERRA's surface air temperature data outperform ERA5 data by more than two degrees.

The temperature of the lower stratosphere (Figure 7) as a whole across the globe is characterized by a cooling during the period from 1980 to 2019. The magnitude of the trend is about −0.15 degrees per decade for MERRA2 data and −0.3 degrees per decade according to ERA5 data. Trends are significant ata 1% significance level. More than half of the total variance is described by short-term variability both in the tropics and on a global scale. The short-term variability of the temperature of the lower stratosphere on a global scale is characterized by the presence of maxima in 1982, 1988, 1992, 1998, 2002, 2009, and

2012–2013 and 2016. At the end of the 20th century, the highest temperature maxima of the lower stratosphere, both in the tropics and on a global scale, fall on the periods after the major volcanic eruptions El Chichon (Mexico, 1982) and Pinatubo (Philippines, 1991). A sharp increase in the content of stratospheric aerosol after these largest volcanic eruptions led to a trapping of the incoming solar radiation in the stratosphere and to its heating. In the XXI, in some years, the opposite phase change in the temperature of the lower stratosphere in the tropics and on average over the globe is noted. In this regard, 2002, 2011, 2012, and 2015 can be noted. The El Niño phenomenon manifests itself in the global average temperature maximums of the lower stratosphere in 1988, 1998, and 2016. In the lower stratosphere of the tropics, no significant connection with the El Niño phenomenon was noted. In contrast to the temperature of the lower troposphere, where the MERRA2 and ERA5 data have a systematic difference of up to 0.5 degrees, in the stratosphere, the data of the two considered reanalyzes practically do not differ.

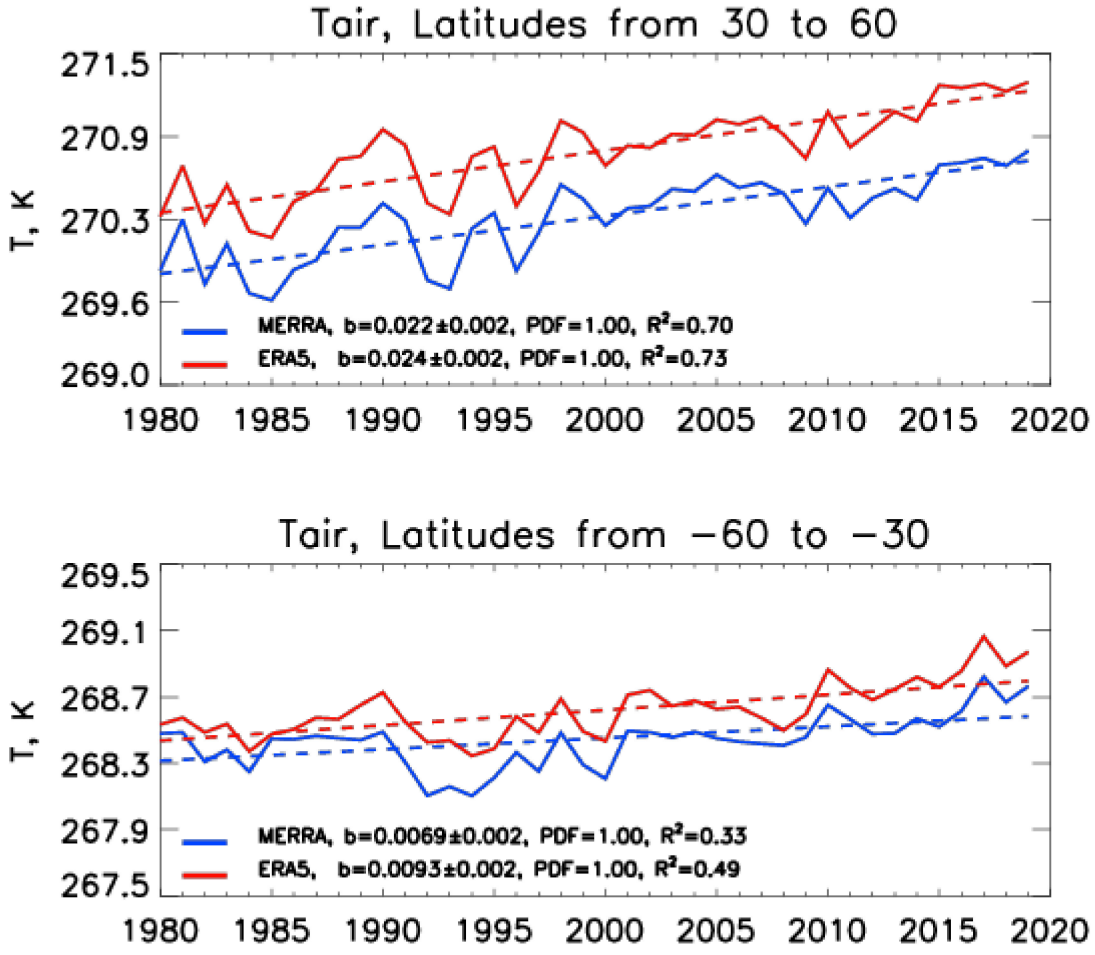

Figure 5. Interannual variability of the lower troposphere air temperature in the midlatitudes of the Northern Hemisphere (**top**) and Southern Hemisphere (**bottom**) based on the reanalysis data MERRA2 (blue) and ERA5 (red) with an assessment of trends (degrees per year) and their significance.

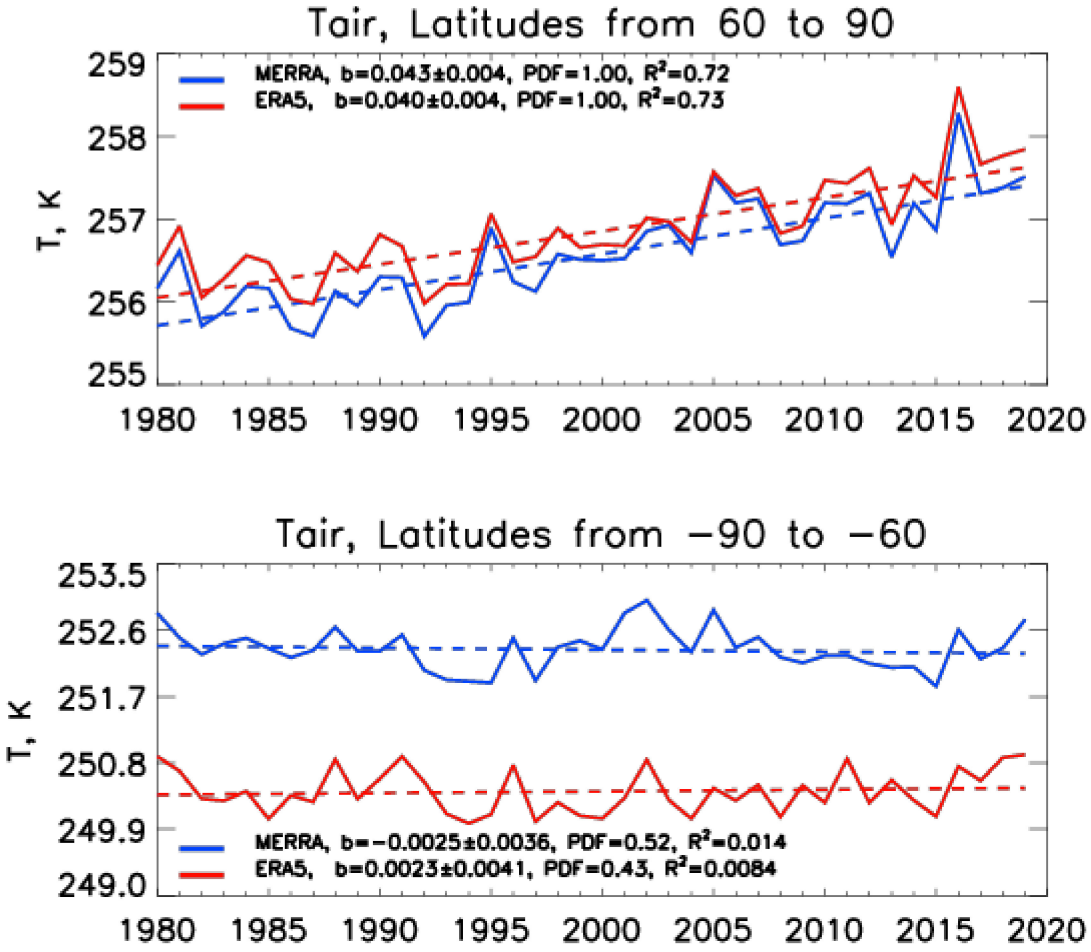

Figure 6. Interannual variability of the lower troposphere air temperature in the polar latitudes of the Northern Hemisphere (**top**) and Southern Hemisphere (**bottom**) based on the reanalysis data MERRA2 (blue) and ERA5 (red) with an assessment of trends (degrees per year) and their significance.

The interannual variability of the temperature of the lower stratosphere in the middle latitudes of the northern (top) and Southern (bottom) Hemispheres according to the MERRA2 and ERA5 reanalysis data is presented in Figure 8. For both hemispheres, the temperature trends in the lower stratosphere are negative at about −0.2 degrees per decade and significant at a 1% significance level. Trends according to ERA5 data are slightly high than trends according to MERRA2 data and amount to −0.2–0.3 degrees per decade. The short-term variability is characterized by the presence of temperature maxima in the lower stratosphere of the middle latitudes of both hemispheres in 1982–1983, 1991–1992, 2005, 2007, 2009, and 2014. An increase in the temperature of the lower stratosphere as a result of large volcanic eruptions at the end of the 20th century is also noted in mid-latitudes, with El Chichon more influencing the temperature in the Northern Hemisphere, and Pinatubo in the Southern Hemisphere. At the same time, the global maximum of 2002 (Figure 7) appears only in the temperature of the lower stratosphere of the middle latitudes of the Southern Hemisphere. As well as for the whole globe and in the tropics, the data on the temperature of the lower stratosphere of middle latitudes differ little for the MERRA2 and ERA5 reanalysis data.

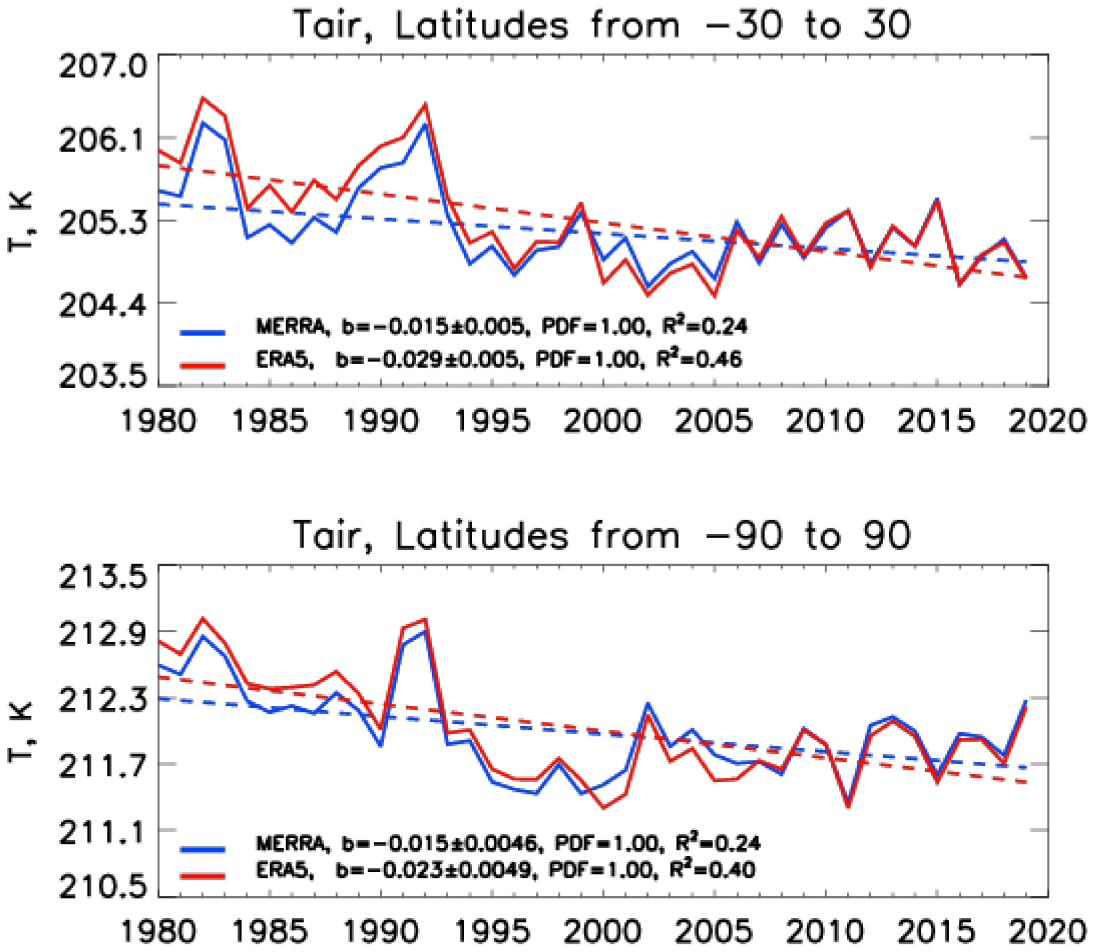

Figure 7. Interannual variability of the lower stratosphere air temperature in tropics(**top**) and globally (**bottom**) based on the reanalysis data MERRA2(blue) and ERA5 (red) with an assessment of trends (degrees per year) and their significance.

The interannual variability of the temperature of the lower stratosphere of the polar regions according to the MERRA2 and ERA5 reanalysis data is shown in Figure 9. Temperature trends are insignificant for the 10% significance level and, at the same time, weakly positive for the Northern Hemisphere and negative for the Southern Hemisphere. More than 95% of total variance is explained by the short-term variability in polar regions. Among the global maximums in the temperature of the lower stratosphere, one can note the maximums of 1991–1992, 1998, 2009, 2012–2013, and 2016, which are manifested in both hemispheres and the maximums of 1998 and 2013 in the polar zone of the Northern Hemisphere and the maximum of 2002 in the Southern Hemisphere. Compared with the phases of the El Niño phenomenon, its most pronounced manifestation in 1998 is characterized by the presence of a temperature maximum in the lower stratosphere of the Arctic and a minimum in the lower stratosphere of the Antarctic. A similar picture is observed in 2010, and in 2016, the maximum temperature of the lower stratosphere appears in the polar lower stratosphere of both hemispheres. In general, it can be noted that, despite the fact that the temperature of the lower stratosphere of the polar regions is characterized by a well-pronounced interannual variability determined by dynamic processes affecting the stability of the polar vortex, such as wave activity and sudden stratospheric warming events, global variability, largely determined by processes in the tropical zone, also manifests itself in polar regions.

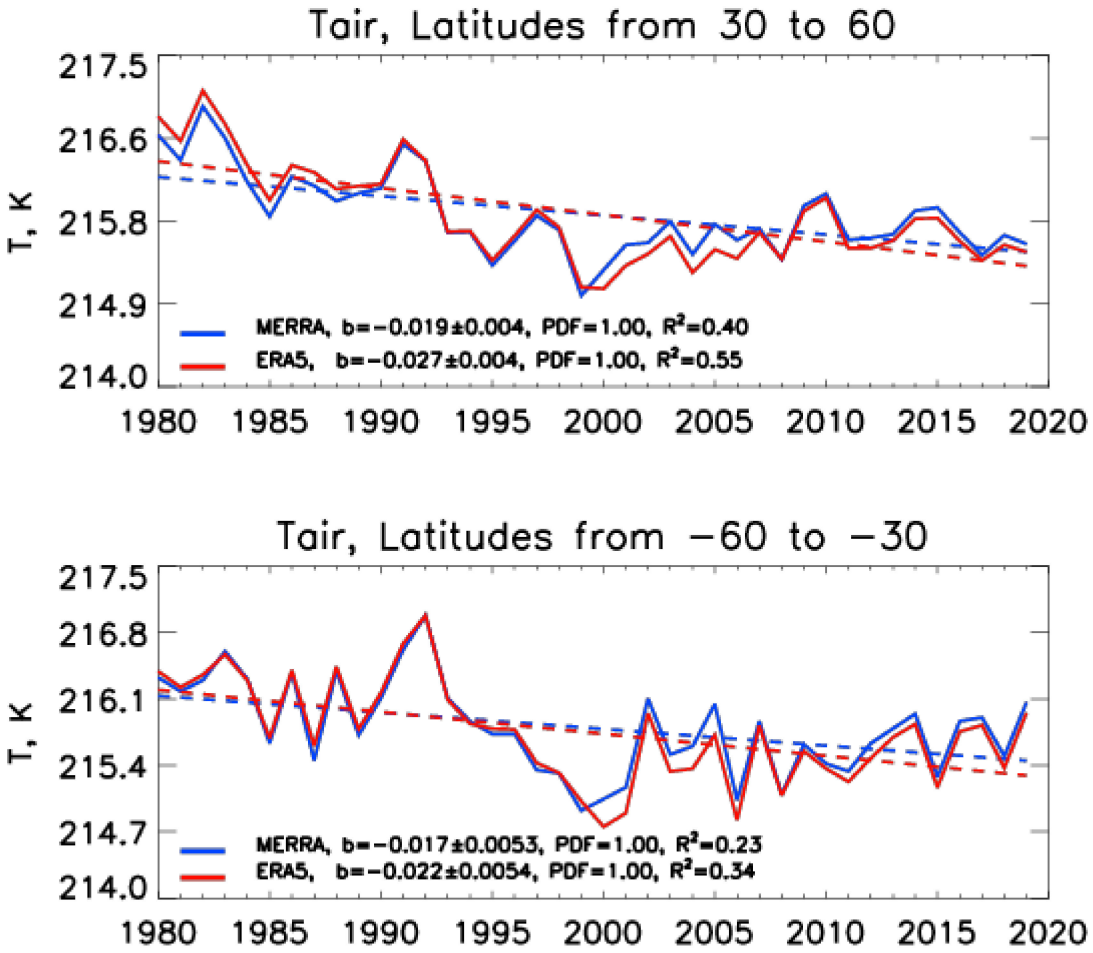

Figure 8. Interannual variability of the lower stratosphere air temperature in the middle latitudes of the Northern Hemisphere (**top**) and Southern Hemisphere (**bottom**) based on the reanalysis data MERRA2 (blue) and ERA5 (red) with an assessment of trends (degrees per year) and their significance.

The short-term variability in the polar regions is largely determined by the dynamics of the polar vortex, the stable state of which leads to a cooling of the polar stratosphere due to the isolation of the polar region from warmer middle latitudes, and the unstable polar vortex leads to a warmer stratosphere [13]. The polar vortex is stable almost every year throughout the entire winter in Antarctica and unstable in the Arctic, which is caused by the higher wave activity in the Arctic, leading to the rapid destruction of the polar vortex that forms at the beginning of winter. Sudden stratospheric warming events (SSW), which regularly occur in the Arctic and rarely in the Antarctic, can also lead to the destruction of the polar vortex. As a result, the average temperature of the lower stratosphere in the Antarctica is 6–7 degrees lower than in the Arctic (Figure 9). Against the background of a higher temperature of the lower stratosphere in the Arctic, individual years with a stable polar vortex (1997 and 2011) stand out, when the temperature of the lower stratosphere is significantly lower than the average climatic temperature (Figure 9, top) during the winter-spring period, which led to the formation of ozone anomalies [53]. In Antarctica, on the contrary, there are several years when the temperature is significantly higher than the average climatic, mainly as a result of the SSW, which was the strongest in 2002 (Figure 9, bottom). It should be noted that during the last decade (2010–2020), the destruction of the polar vortex, leading to a sharp increase in the temperature of the lower stratosphere, occurs in Antarctica more often than in previous decades (Figure 9, bottom).

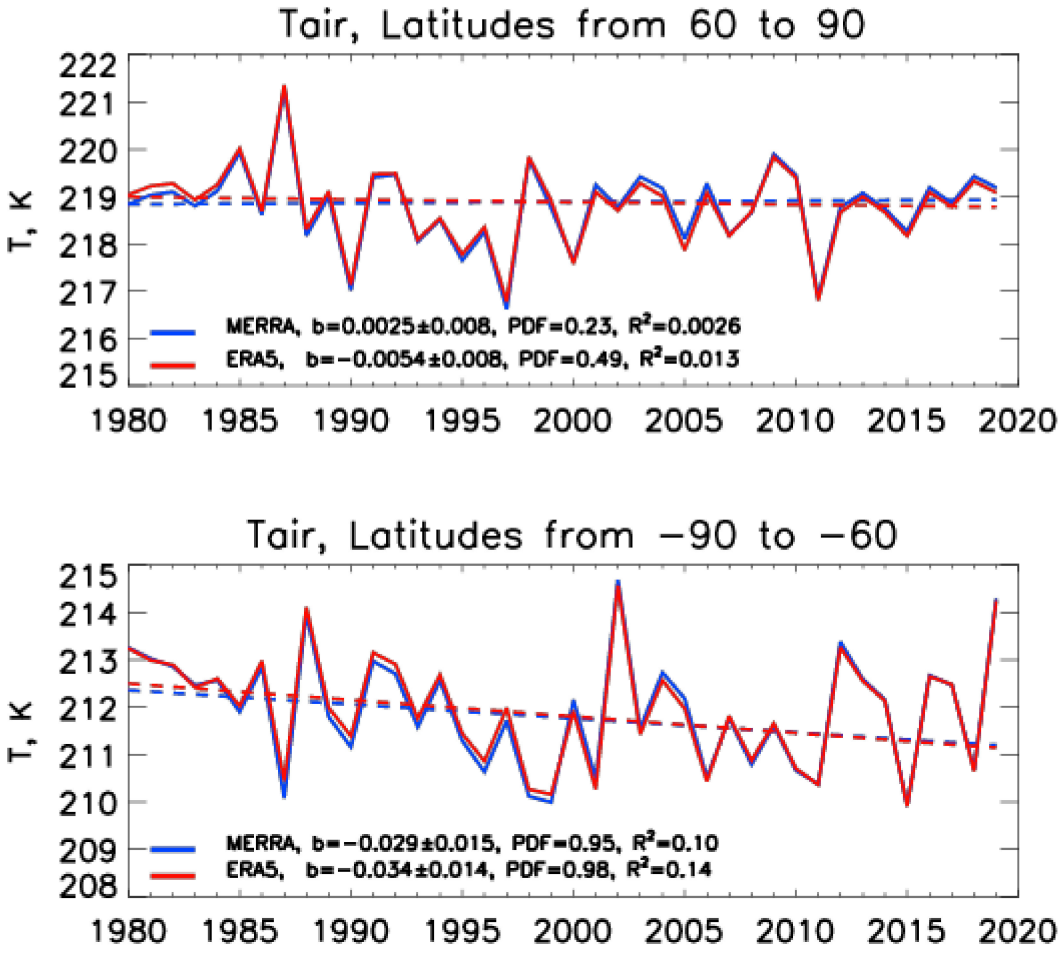

Figure 9. Interannual variability of the lower stratosphere air temperature in the polar latitudes of the Northern Hemisphere (**top**) and Southern Hemisphere (**bottom**) based on the reanalysis data MERRA2 (blue) and ERA5 (red) with an assessment of trends (degrees per year), their significance, and coefficient of determination.

4. Numerical Modeling of the Simultaneous Influence of Sea Surface Temperature Variability and an Increase in the Content of Greenhouse Gases on the Atmospheric Temperature during 1979–2019

To numerically simulate the simultaneous effect of sea surface temperature variability and an increase in the content of greenhouse gases on the atmospheric temperature, the chemistry-climate model of the INM RAS–RSHU was used. The calculations were performed for the period from 1979 to 2019 [52,54]. To take into account the influence of greenhouse gases for this period, the variability of their surface concentrations was set in accordance with the IPCC Climate System Scenario Tables [50,54,65,66], and to take into account the effect of sea surface temperature (SST) and sea ice coverage (SIC), the reanalysis data were used adopted to the CCM grid. The variability of the chemical composition of the atmosphere was taken into account by setting the surface concentrations of chemically active components in accordance with the data of WMO-UNEP 2018. In the baseline scenario, two calculations were performed with SST and SIC from two different re-analysis data: Met Office and ERA5. To assess the impact of climatic changes over the past 40 years on the temperatures of the lower troposphere and lower stratosphere, the model simulated values of the temperatures of the lower troposphere (925 hPa) and lower stratosphere (20 hPa), averaged over 11 years (first and last solar cycle) at the beginning of the 11-year climatic period (solar cycle) (1980–1990) and at the end of the climatic period (2009–2019) were compared. The first period (1980–1990) is characterized by lower values of SST, atmospheric loading of greenhouse gases (CO_2, CH_4, N_2O), and emissions

of ozone-depleting substances (ODS) than in the second period (2009–2019). The results of the model calculations were compared with the re-analysis data from MERRA2 and ERA5. The difference between the investigated characteristics is shown in Figure 10.

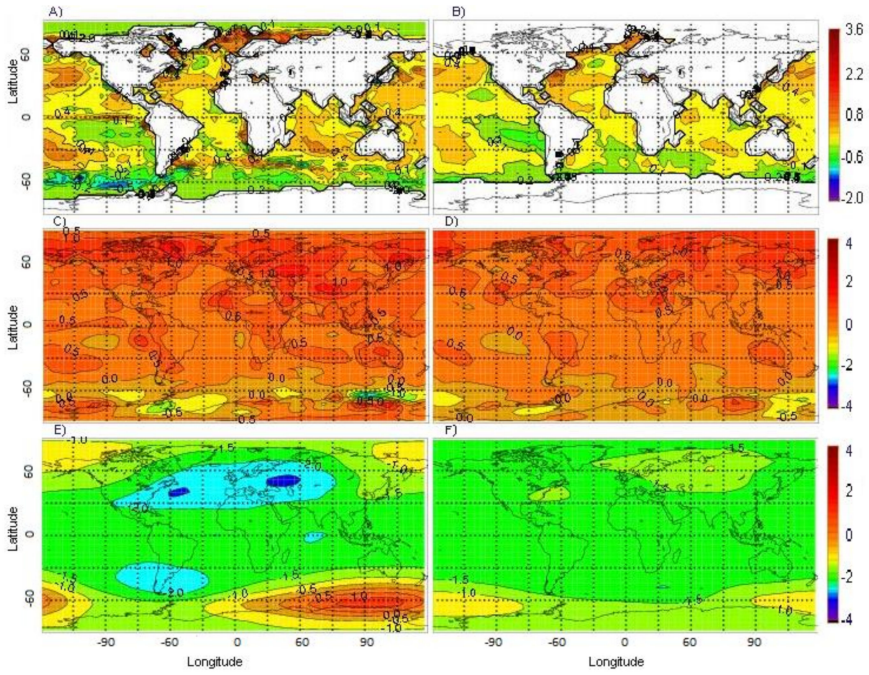

Figure 10. The difference between the averaged over the periods 2009–2019 and 1980–1990 sea surface temperature according to reanalysis data (**A**,**B**), as well as air temperature at the level of 925 hPa (**C**,**D**) calculated on the chemistry-climate model (CCM), air temperature at 20 hPa (**E**,**F**). The left column corresponds to sea-surface temperature (SST) in the lower boundary based on ERA5 data and the right column is for Met Office SST in the model lower boundary.

The results of the calculations performed with the CCM showed that in the lower troposphere in the Arctic there is a much stronger warming than in the Antarctic, which corresponds to the well-known hypothesis of "Arctic amplification". For both SST and SIC reanalysis sets, calculations with a chemistry-climate model show a maximum increase in the temperature of the lower troposphere in the Greenland sector, as well as in the eastern part of Siberia, and a decrease in SST and air temperature west of South America. The reanalysis data (Figure 11) also support the hypothesis of Arctic amplification and local cooling in the Antarctic lower troposphere.

In the Antarctic, in contrast to the Arctic, according to the results of calculations with a chemistry-climate model and according to reanalysis data, the warming in the lower troposphere is the lowest compared to other latitudes, and even a cooling is noted in some areas of the southern polar zone. The smallest changes in the surface temperature are obtained in the calculations with the CCM using the SST and SIC from the data of the ERA5 reanalysis. The significant difference between the two polar regions suggests that, on the one hand, the dynamical factors that determine the difference between the polar zones of the northern and Southern Hemispheres play a critical role in the variability of the temperature of the lower troposphere in the Arctic and Antarctic, and, on the other hand, the ability of chemical-climatic model with a given variability of influencing parameters to describe the observed features of temperature variations in the surface layer of the polar atmosphere.

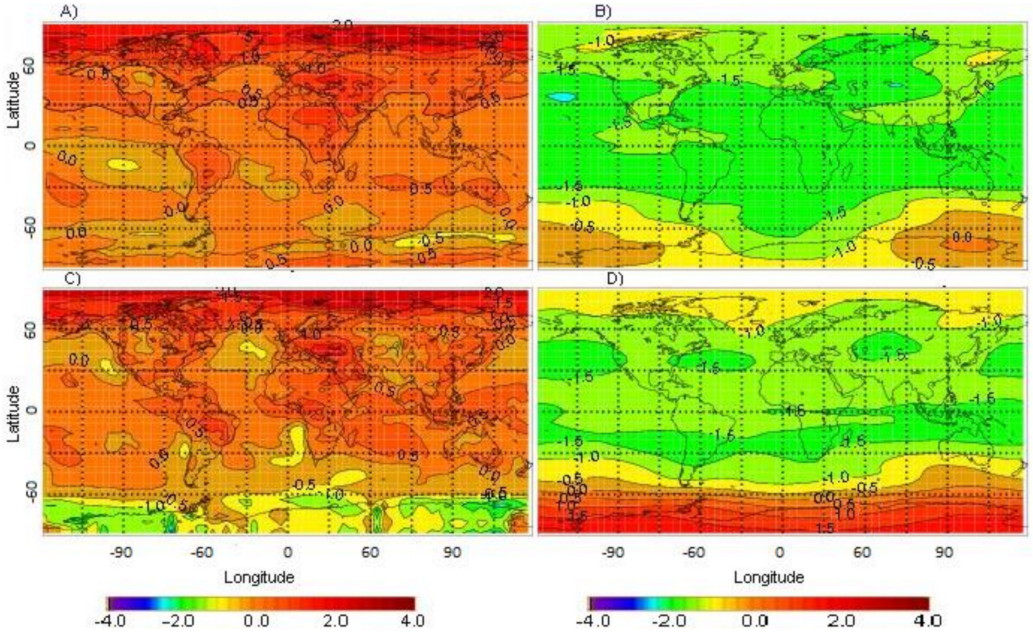

Figure 11. The difference in values averaged over the periods from 2009 to 2019 and from 1980 to 1990: According to the reanalysis of ERA5 (**A**,**B**), MERRA2 (**C**,**D**). The left column is the air temperature at 925 hPa, the right column is the air temperature at 20 hPa.

In the lower stratosphere, the results of model calculations, as well as the reanalysis data, show, in contrast to the lower troposphere, a cooling in most of the globe. At the same time, as well as in the surface layer, there is a significant difference between the northern and southern polar zones. While in Antarctica the least cooling of the stratosphere, and in some places even warming, is recorded in comparison with other latitudes, in the Arctic, there is a significant difference between the western and eastern parts. In the eastern part of the polar zone of the Northern Hemisphere, the results of model calculations show the maximum cooling of the stratosphere for the entire globe, and in the western zone there is minimum cooling, while in the north of the American continent and Greenland, there is even warming of the stratosphere. At the same time, while in the lower troposphere the use of different reanalysis data for SST and SIC did not lead to a significant difference in the results of model calculations, in the stratosphere, the results of modeling temperature variability for different SST and SIC differ significantly, especially for the polar regions. This suggests that due to the important role of dynamic processes, which are significantly influenced by the exchange of heat, mass, and angular momentum between the ocean and the atmosphere, the variability of the SST and SIC is important not only for the troposphere, which directly borders the ocean, but also for the stratosphere, which is more than 10 km away from the ocean. It should be noted that the ERA5 and MERRA2 reanalysis data also differ more in the stratosphere than in the troposphere, both among themselves and with the results of model calculations with different SST.

Numerical modeling of the effect of the sea surface temperature and sea ice coverage on the variability of the composition and structure of the stratosphere at different latitudes with different data from the reanalysis of SST and SIC showed that these parameters play an important role for the temperature not only in the troposphere, but in the stratosphere as well.

For an in-depth study of the influence of SST and SIC on the content of atmospheric gases in the Arctic and Antarctic and highlighting their influence on the variability of temperature against the background of other influencing factors, additional calculations were carried out for three additional scenarios with the assignment of SST and SIC according to the Met Office reanalysis data. In the first scenario, the values of carbon dioxide loading and SST/SIC were fixed at 1979 level. This scenario model simulation was performed to assess

the impact of other but CO_2 and SST/SIC changes during 1979–2019. Among these factors are emissions of other greenhouse (CH_4 and N_2O) and ozone-depleting gases, aerosols, and solar activity. In the second additional model experiment, the CO_2 year to year variability in accordance with the IPCC Climate System Scenario Tables was taken into account, while the SST and SIC remained at the 1979 level. The purpose of this model experiment was to assess the separate effect of an increase in carbon dioxide content on tropospheric and stratospheric temperatures. In the third additional scenario, carbon dioxide loading was fixed at the 1979 level, while SST and SIC were changed according to Met Office data. This experiment made it possible to evaluate the separate SST/SIC impact on the atmospheric circulation and, through it, on the tropospheric and stratospheric temperature.

In the experiment with fixed CO_2 and SST/SIC (Figure 12A,B) in the lower troposphere, the temperature increased fairly uniformly across the globe with the centers of maximum increase in the Arctic and Subarctic and cooling in the Antarctic (Figure 12A). In the stratosphere, at the same time, there is a slight uniform cooling within −0.5 degrees in tropical and middle latitudes, as well as centers of temperature decrease of more than −1.5 degrees in Eastern Siberia and the Far East, insignificant temperature changes in Northern Europe and Antarctica (Figure 12B). In addition, in some regions of Antarctica, under the influence of factors not related to CO_2 and SST/SIC, an increase in the temperature of the lower stratosphere by more than 0.5 degrees is noted. The results of this model experiment showed that many local features of changes in temperature in polar regions, in particular in the north of the American continent, Siberia, and Antarctica, are not a consequence of changes in the content of CO_2 and SST/SIC but are associated with other global factors and features of local variability, in particular, circulation in the regions.

In the experiment with varying CO_2 emissions and fixed SST/SIC, the change in the temperature of the lower troposphere (Figure 12C) is similar to that noted in the first experiment (Figure 12A). At the same time, warming due to an increase in CO_2 loading is slightly higher than due to other greenhouse gases and other factors, and the regions of maximum warming and cooling are also located in the Arctic and Antarctic. Since the content of carbon dioxide increases uniformly over the entire globe, such localization may be a consequence of local dynamic conditions superimposed on the change in the radiation balance with an increase in the content of CO_2. In the lower stratosphere, an increase in carbon dioxide content leads to a significant cooling with maximum values of up to −4 degrees in the Antarctic and more than −2 degrees in certain regions of the Arctic (Figure 12D).

In the scenario with fixed CO_2 and varying SST/SIC in the lower troposphere, the air temperature increases more than in the previous scenarios (Figure 12E). The greatest warming is noted in the Arctic (Arctic amplification), but in Antarctica, for this scenario, the temperature of the lower troposphere increases more than in middle and tropical latitudes. In the lower stratosphere (Figure 12G), a slight cooling persists, similar to that noted in the first scenario, but in addition, areas of temperature decrease in the tropics and subtropics appear. At the same time, warming in some regions of Antarctica increases, while in the Arctic and Subarctic, the area of weak temperature changes increases in comparison with the first scenario. In addition, areas of increased temperature appear in eastern Eurasia and Alaska.

In the baseline scenario, when all factors are taken into account (Figure 12G,H), the Arctic amplification is well expressed in the lower troposphere, which manifests itself in maximum warming in the Arctic and minimum warming, and even cooling in some regions, in Antarctica. Thus, the results of numerical experiments with the CCM revealed that only taking into account the simultaneous influence of the CO_2 and SST/SIC variability makes it possible to sufficiently reliably reproduce the observed changes in the temperature of the lower troposphere and the differences between the northern and Southern Hemispheres (Figure 12G). In the lower stratosphere, for the baseline scenario, SST/SIC variability partially compensates the cooling due to increased CO_2 (Figure 12D,H).

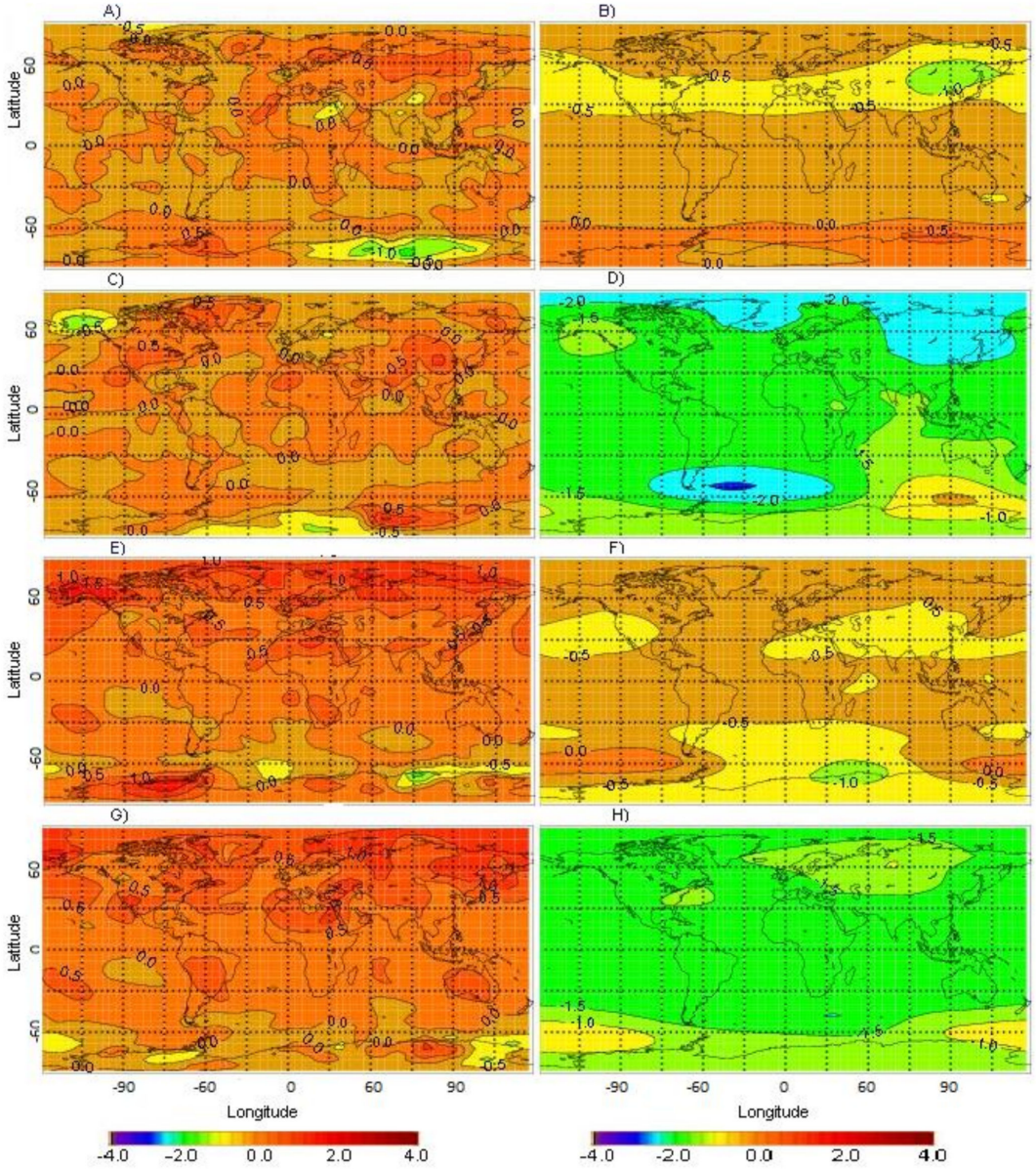

Figure 12. The difference between the CCM simulation results (according to the SST and sea ice coverage (SIC) Met office data), averaged over the periods from 2009 to 2019 and from 1980 to 1990: In experiments with fixed values of SST and CO_2 at the 1979 level (**A**,**B**), with fixed SST at 1979 level (**C**,**D**), with CO_2 fixed at 1979 (**E**,**F**) and baseline (**G**,**H**). The left column is the air temperature at the level of 925 hPa and the right column is the air temperature at the level of 20 hPa.

5. Discussion

The results of numerical experiments have shown that the air temperature in the lower troposphere is basically determined by the variability of SST. Correlation analysis confirms this conclusion. The correlation coefficient between SST anomaly and air temperature anomaly at the level of 925 hPa is 0.85, both for the reanalysis data and for the simulation results. If we estimate the correlation coefficients for some regions, then for the Pacific Ocean it is equal to 0.86 and for the tropical part of the Pacific Ocean (ENSO region, 5° S–5° N, 170° W–120° W) it is 0.90. For the Atlantic Ocean it is 0.82 and for the Indian Ocean it is 0.8. For the Arctic and Antarctic, it is 0.81 and 0.7, respectively. For areas over land, the correlation is less—the correlation coefficients are 0.65 and 0.7 for the troposphere over Eurasia and America. The correlation between the SST anomaly in the El Niño region and the air temperature anomaly in the troposphere of the Arctic and Antarctic are −0.4

and −0.03, respectively, and the air temperature anomaly in the Northern and Southern Hemispheres—−0.4 and 0.17, respectively.

In the stratosphere, the SST anomaly variability does not significantly affect the air temperature anomaly—the correlation coefficients range from 0.2 to 0.3. For the Northern Hemisphere, the correlation coefficient between SST anomaly and air temperature anomaly in the stratosphere is −0.37. At the same time, in El Niño years, the correlation coefficients between SST anomaly and air temperature anomaly in the Arctic stratosphere are 0.4–0.5, in La Niña years—0.4, in years of the neutral phase—from −0.45 to 0.4. For the Southern Hemisphere, the correlation coefficient is 0.2.

As for the influence of the level of carbon dioxide on air temperature, in the troposphere it has a significant effect on changes in air temperature. So, the correlation coefficient between the concentration of carbon dioxide and air temperature anomaly is 0.65 for the whole planet. The largest value of this coefficient was obtained for the Northern Hemisphere—the coefficient is 0.75, which is explained by the presence of a large number of carbon dioxide sources, mainly of anthropogenic origin [16–18]. For the Southern Hemisphere, it is 0.65. For the stratosphere, the correlation coefficient is −0.5—the correlation is negative, which corresponds to the cooling of the stratosphere, while it is more significant than between the air temperature in the stratosphere and the SST. At the same time, significant differences in the distribution of air temperature in the stratosphere for experiments with fixed and non-fixed CO_2 levels indicates a greater significance of changes in the level of CO_2 for the stratosphere than changes in SST [33,34,52].

Comparison of the results of additional scenarios of model calculations with the baseline scenario, in which the variability of all influencing parameters is set, allows us to conclude that, due to the peculiarities of circulation in the polar regions, an increase in the carbon dioxide content leads to less cooling of the stratosphere in the Arctic compared to other latitudes and more cooling in the Antarctic, if we do not take into account the influence of variability in sea surface temperature and ice surface area on circulation in the north polar region. The cumulative effect of climatic changes associated with the influence of the variability of carbon dioxide and the temperature of the sea surface and the area of ice coverage leads to the localization of the circumpolar vortex, as a result of which in the eastern hemisphere, especially in northern Siberia, the strongest cooling of the stratosphere occurs [33,34,70].

6. Conclusions

Reanalysis data, as well as numerical simulations with a global chemistry-climate model of the lower and middle atmosphere were used to study the effect of sea surface temperature and carbon dioxide variability on the temperature of the lower troposphere and low stratosphere during the period from 1980 to 2019.

Analysis of sea surface temperature trends based on reanalysis data revealed that, on average, a significant positive SST trend of about 0.01 degrees per year is observed over the globe. At the same time, in the middle latitudes of the Northern Hemisphere, the trend (about 0.02 degrees per year) is 2 times higher than the global average, and 5 times higher than in the Southern Hemisphere (about 0.004 degrees per year). At polar latitudes, opposite SST trends are observed in the Arctic (positive) and Antarctic (negative). The short-term variability of the SST on average over the globe coincides with a good degree of accuracy with the phases of the Southern Oscillation in the tropics, while in the middle and polar latitudes, the phases of the Southern Oscillation are noticeable for the most powerful El Niño and La Niña phenomena in the short-period variability in the Northern Hemisphere and are practically invisible in the Southern Hemisphere.

The air temperature in the lower troposphere is characterized by a positive significant trend on average over the globe (about 0.015 degrees per year), slightly exceeding the global SST trend. For some latitudinal areas, the maximum trend in the temperature of the lower troposphere is noted in the Arctic (about 0.45 degrees per year), and the minimum—in the Antarctic (insignificant negative trend). In the middle latitudes of the

Northern Hemisphere, the trend in the temperature of the lower troposphere (about 0.02 degrees per year) is almost three times higher than the trend in the temperature of the lower troposphere of the Southern Hemisphere (about 0.007 degrees per year). The short-term variability of the mean global temperature of the lower troposphere is in good agreement with the phases of the southern oscillation, which has a tropical nature. At the same time, in middle and, especially, polar latitudes, the dependence of short-period fluctuations in the temperature of the lower troposphere on the phases of the southern oscillation is much less than for tropical latitudes and on average over the globe. The reanalysis data for the temperature of the lower troposphere have systematic differences: Everywhere, except for the Antarctic region, the values according to the ERA5 data exceed the values according to the MERRA2 data.

In the lower stratosphere, a significant cooling is observed during 1980–2019 period, i.e., the direction of the temperature trend is opposite to its trend in the lower troposphere [32,33,70]. The cooling rate in the lower stratosphere on a global scale is about −0.02 degrees per year, and these values are close both in the tropical zone and in the middle latitudes of both hemispheres and in Antarctica. Only in the lower stratosphere of the Arctic is there an insignificant, weakly positive trend. The short-term variability of the temperature of the lower stratosphere is less dependent on the phases of the southern oscillation, and to a greater extent is determined by the circulation features of different hemispheres and latitudinal zones. The reanalysis data for the temperature of the lower stratosphere differ much less from each other than was observed in the lower troposphere. Only a slightly lower linear trend coefficient can be noted for ERA5 data compared to MERRA2 data.

The results of model calculations with a global chemistry-climate model demonstrated that in the lower troposphere, an increase in air temperature is determined to a greater extent by a change in the temperature of the sea surface and its ice coverage than by an increase in the content of carbon dioxide [33,34,70]. At the same time, the Arctic amplification is determined by the cumulative effect of both the sea surface temperature and sea ice coverage, and an increase in the content of greenhouse gases. On the other hand, if CO_2 changes are not taken into account, then the air temperature in the stratosphere will change little. Thus, the study showed that changes in the CO_2 content are a significant factor for the observed cooling of the stratosphere, the fixation of which makes the temperature of the stratosphere almost constant during 1980–2019, and the change in SST has only an insignificant effect on it.

Author Contributions: Conceptualization, S.P.S. and V.Y.G.; methodology, S.P.S. and V.Y.G.; Formal analysis, A.R.J.; data curation, A.R.J.; writing—original draft preparation, A.R.J.; writing—review and editing, S.P.S.; visualization, A.R.J. All authors have read and agreed to the published version of the manuscript.

Funding: This research workis executed at the Russian State Hydrometeorology University within the limits of the state task of the Ministry of higher education and a science of the Russian Federation (project no. FSZU-2020-0009). Change of gas structure of an atmosphere of Arctic regions and Subarctic region was simulated with a support of the Russian Scientific Foundation (project 19-17-00198). Interaction between stratosphere and troposphere was studied under Russian Foundation for Basic Research (project 20-55-53039). Part of this study was performed in the SPbSU Ozone Layer and Upper Atmosphere Research Laboratory, which is supported by the Ministry of Science and Higher Education of the Russian Federation.

Institutional Review Board Statement: The study was conducted according to the guidelines of the Declaration of Helsinki, and approved by the Institutional Review Board (or Ethics Committee) of the Russian State Hydrometeorological University.

Informed Consent Statement: Informed consent was obtained from all subjects involved in the study.

Data Availability Statement: Reanalysis data are available from RSHU data service (ra.rshu.ru/ra (accessed on 23 March 2021)). Results of model calculations are available upon request (smyshl@rshu.ru).

Acknowledgments: We would like to thank European Centre for Medium-Range Weather Forecasts (ECMWF) for providing the ERA5 Data Set, NASA for providing the MERRA2 Data Set, and Met Office Hadley Centre for providing sea surface temperature and sea ice coverage data. The authors are grateful to the two anonymous referees for their attention to the manuscript and helpful and constructive comments.

Conflicts of Interest: The authors declare no conflict of interest.

References

1. Bondarenko, A.L.; Zhmur, V.V. Nature and forecasting possibility of the El-Nino/La-Nina phenomenon. *Russ. Meteorol. Hydrol.* **2004**, *11*, 26–35.
2. Achuta Rao, K.; Sperber, K.R. Simulation of the El Nino Southern Oscillation: Results from the coupled model intercomparison project. *Clim. Dyn.* **2002**, *19*, 191–209.
3. Bendik, A.B.; Jakivlev, V.N. About rapprochement of approaches to understanding of El-Nino—La-Nina phenomenon. *Vestn. Russ. State Univ. Kanta.* **2010**, *1*, 57–64. (In Russian)
4. Astaf'eva, N.M.; Raev, M.D.; Komarova, N.J. Regional geterogenety of climate changes. Modern problems of remote sounding of the Earth from space. Physical bases, methods and technologies of monitoring of the environment, potentially dangerous phenomena and objects. *Collect. Artic.* **2008**, *5*, 1–12. (In Russian)
5. Guilyardi, E.; Wittenberg, A.; Fedorov, A.; Collins, M.; Wang, C.; Capotondi, A.; Oldenborgh, G.J.; van Stockdale, T. Understanding El Nino in ocean-atmosphere general circulation models. Progress and Challenges. *Am. Meteorogical Soc.* **2009**, *90*, 325–340. [CrossRef]
6. Taylor, K.E.; Williamson, D.; Zwiers, F. The sea surface temperature and sea-ice concentration boundary conditions for AMIP II simulations. In *Program for Climate Model Diagnosis and Intercomparison*; Report No. 60.; Lawrence Livermore National Laboratory, University of California: Livermore, CA, USA, 2000.
7. Jadin, E.A. Interannual variations of ozone above Europe and anomalies of ocean temperatures in Atlantic. *Meteorol. Hydrol.* **1992**, *7*, 22–26. (In Russian)
8. Jadin, E.A. Long-periodic cyclicity of temperature of ocean surface, temperature of low stratosphere and ozone in moderated latitudes. *Meteorol. Hydrol.* **1993**, *5*, 52–59. (In Russian)
9. Jadin, E.A. Arctic oscillation and interannual variations of temperature of Atlantic and Pacific oceans. *Meteorol. Hydrol.* **2001**, *8*, 28–40. (In Russian)
10. Hu, D.; Tian, W.; Xie, F.; Shu, J.; Dhomse, S. Effects of meridional sea surface temperature changes on stratospheric temperature and circulation. *Adv. Atmos. Sci.* **2014**, *31*, 888–900. [CrossRef]
11. Bell, C.; Gray, L.; Charlton-Perez, A.; Joshi, M.; Scaife, A. Stratospheric Communication of El Ninõ Teleconnections to European Winter. *J. Clim.* **2009**, *22*, 4083–4096. [CrossRef]
12. Manatsa, D.; Mukwada, G. A connection from stratospheric ozone to El Niño-Southern Oscillation. *Sci. Rep.* **2017**, *7*, 5558. [CrossRef]
13. Smyshlyaev, S.P.; Pogoreltsev, A.I.; Galin, V.J. Influence of wave activity on gaseous composition of stratosphere of polar regions. *Geomagn. Aeron.* **2016**, *56*, 102–116. [CrossRef]
14. Newman, P.A.; Nash, E.R.; Rosenfield, J.E. What controls the temperature of the Arctic stratosphere during the spring? *J. Geophys. Res.* **2001**, *106*, 19999–20010. [CrossRef]
15. Chipperfield, M.P.; Jones, R.L. Relative influences of atmospheric chemistry and transport on Arctic ozone trends. *Nature* **1999**, *400*, 551–554. [CrossRef]
16. Solomon, S.; Dahe, Q.; Manning, M. (Eds.) *Intergovernmental Panel on Climate Change (IPCC), Climate Change 2007*; Cambridge University Press: New York, NY, USA, 2007; p. 996.
17. Hansen, J.; Sato, M.; Ruedy, R.; Lacis, A.; Oinas, V. Global warming in the twenty-first century: Analternative scenario. *Proc. Natl. Acad. Sci. USA* **2000**, *97*, 9875–9880. [CrossRef]
18. Prentice, I.C.; Farquhar, G.D.; Fasham, M.J.R.; Goulden, M.L.; Heimann, M.; Jaramillo, V.J.; Kheshgi, H.S.; LeQuéré, C.; Scholes, R.J.; Wallace, D.W. The carbon cycle and atmospheric carbon dioxide. In *Climate Change 2001: The Scientific Basis—Third Assessment Report of the Intergovernmental Panel on Climate Change*; IPCC, Ed.; Cambridge University Press: Cambridge, UK, 2001; pp. 183–238.
19. Stevenson, S.; Fox-Kemper, B. Understanding the ENSO–CO_2 Link Using Stabilized Climate Simulations. *J. Clim.* **2012**, *25*, 7917–7936. [CrossRef]
20. Ropelewski, F.C.; Halpert, M.S. Quantifying Southern Oscillation–precipitation relationships. *J. Clim.* **1996**, *9*, 1043–1059. [CrossRef]
21. Rajagopalan, B.; Lall, U. Interannual variability in western US precipitation. *J. Hydrol.* **1998**, *210*, 51–67. [CrossRef]
22. Whetton, P.; Adamson, D.; Williams, M. Rainfall and river flow variability in Africa, Australia and east Asia linked to El Nino Southern Oscillation. *Geol. Soc. Aust. Proc. Symp.* **1990**, *1*, 71–82.
23. AchutaRao, K.; Sperber, K.R. ENSO simulation in coupled ocean-atmosphere models: Are the current models better? *Clim. Dyn.* **2006**, *27*, 1–15. [CrossRef]
24. Guilyardi, E. El Nino–mean state–seasonal cycle interactions in a multi-model ensemble. *Clim. Dyn.* **2006**, *26*, 329–348. [CrossRef]

25. Collins, M.; An, S.-I.; Cai, W.; Ganachaud, A.; Guilyardi, E.; Jin, F.-F.; Jochum, M.; Lengaigne, M.; Power, S.; Timmermann, A. The impact of global warming on the tropical Pacific Ocean and El Niño. *Nat. Geosci.* **2010**, *3*, 391–397. [CrossRef]
26. McPhaden, M.J.; Busalacchi, A.J.; Cheney, R.; Donguy, J.-R.; Gage, K.S.; Halpern, D.; Ji, M.; Julian, P.; Meyers, G.; Mitchum, G.T.; et al. The Tropical Ocean-Global Atmosphere observing system: A decade of progress. *J. Geophys. Res. Space Phys.* **1998**, *103*, 14169–14240. [CrossRef]
27. Smith, T.; Reynolds, R. Improved extended reconstruction of SST (1854–1997). *J. Clim.* **2004**, *17*, 2466–2477. [CrossRef]
28. Rayner, N.A.; Brohan, P.; Parker, D.E.; Folland, C.K.; Kennedy, J.J.; Vanicek, M.; Ansell, T.J.; Tett, S.F.B. Improved Analyses of Changes and Uncertainties in Sea Surface Temperature Measured In Situ since the Mid-Nineteenth Century: The Had SST2 Dataset. *J. Clim.* **2006**, *19*, 446–469. [CrossRef]
29. Ropelewski, C.F.; Halpert, M.S. North American Precipitation and Temperature Patterns Associated with the El Niño/Southern Oscillation (ENSO). *Mon. Weather. Rev.* **1986**, *114*, 2352–2362. [CrossRef]
30. Trenberth, K.; Hurrell, J.W. Decadal atmosphere-ocean variations in the Pacific. *Clim. Dyn.* **1994**, *9*, 303–319. [CrossRef]
31. Wittenberg, A.T. Are historical records sufficient to constrain ENSO simulations? *Geophys. Res. Lett.* **2009**, *36*. [CrossRef]
32. Stevenson, S. Significant changes to ENSO strength and impacts in the twenty-first century: Results from CMIP5. *Geophys. Res. Lett.* **2012**, *39*, L17703. [CrossRef]
33. Steiner, A.K.; Ladstädter, F.; Randel, W.J.; Maycock, A.C.; Fu, Q.; Claud, C.; Gleisner, H.; Haimberger, L.; Ho, S.-P.; Keckhut, P. Observed temperature changes in the troposphere and stratosphere from 1979 to 2018. *J. Clim.* **2020**, *33*, 1–72. [CrossRef]
34. Maycock, A.C.; Randel, W.J.; Steiner, A.K.; Karpechko, A.Y.; Christy, J.; Saunders, R.; Thompson, D.W.J.; Zou, C.-Z.; Chrysanthou, A.; Abraham, N.L. Revisiting the Mystery of Recent Stratospheric Temperature Trends. *Geophys. Res. Lett.* **2018**, *45*, 9919–9933. [CrossRef] [PubMed]
35. Shine, K.P.; Bourqui, M.S.; Forster, P.M.D.F.; Hare, S.H.E.; Langematz, U.; Braesicke, P.; Grewe, V.; Ponater, M.; Schnadt, C.; Smith, C.A.; et al. A comparison of model simulated trends in stratospheric temperatures. *Q. J. R. Meteorol. Soc.* **2003**, *129*, 1565–1588. [CrossRef]
36. Ramaswamy, V.; Chanin, M.-L.; Angell, J.; Barnett, J.; Gaffen, D.; Gelman, M.; Keckhut, P.; Koshelkov, Y.; Labitzke, K.; Lin, J.-J.R. Stratospheric temperature trends: Observations and model simulations. *Rev. Geophys.* **2001**, *39*, 71–122. [CrossRef]
37. Karl, T.R.; Hassol, S.J.; Miller, C.D.; Murray, W.L. (Eds.) 2006: Temperature Trends in the Lower Atmosphere: Steps for Understanding and Reconciling Differences. In *A Report by the Climate Change Science Program and the Subcommittee on Global Change Research*; US Climate Change Program: Washington, DC, USA, 2006.
38. Trenberth, K.E.; Anthes, R.A.; Belward, A.; Brown, O.B.; Habermann, T.; Karl, T.R.; Running, S.; Ryan, B.; Tanner, M.; Wielicki, B. Challenges of a Sustained Climate Observing System. In *Climate Science for Serving Society*; Asrar, G.R., Hurrell, J.W., Eds.; Springer: Berlin/Heidelberg, Germany, 2013; pp. 13–50.
39. Titchner, H.A.; Thorne, P.W.; McCarthy, M.P.; Tett, S.F.B.; Haimberger, L.; Parker, D.E. Critically Reassessing Tropospheric Temperature Trends from Radiosondes Using Realistic Validation Experiments. *J. Clim.* **2009**, *22*, 465–485. [CrossRef]
40. Christy, J.R.; Norris, W.B.; Spencer, R.W.; Hnilo, J.J. Tropospheric temperature change since 1979 from tropical radiosonde and satellite measurements. *J. Geophys. Res. Space Phys.* **2007**, *112*, D06102. [CrossRef]
41. Fu, Q.; Manabe, S.; Johanson, C.M. On the warming in the tropical upper troposphere: Models versus observations. *Geophys. Res. Lett.* **2011**, *38*, 26. [CrossRef]
42. Mitchell, D.M.; Thorne, P.W.; Stott, P.A.; Gray, L.J. Revisiting the controversial issue of tropical tropospheric temperature trends. *Geophys. Res. Lett.* **2013**, *40*, 2801–2806. [CrossRef]
43. Thompson, D.W.J.; Seidel, D.J.; Randel, W.J.; Zou, C.-Z.; Butler, A.H.; Mears, C.A.; Osso, A.; Long, C.; Lin, R. The mystery of recent stratospheric temperature trends. *Nat. Cell Biol.* **2012**, *491*, 692–697. [CrossRef]
44. Po-Chedley, S.; Fu, Q. Discrepancies in tropical upper tropospheric warming between atmospheric circulation models and satellites. *Environ. Res. Lett.* **2012**, *7*, 13. [CrossRef]
45. Spencer, R.W.; Christy, J.R.; Braswell, W.D. UAH Version 6 global satellite temperature products: Methodology and results. *Asia Pac. J. Atmos. Sci.* **2017**, *53*, 121–130. [CrossRef]
46. Stone, P.H.; Carlson, J.H. Atmospheric Lapse Rate Regimes and Their Parameterization. *J. Atmos. Sci.* **1979**, *36*, 415–423. [CrossRef]
47. Santer, B.D.; Solomon, S.; Pallotta, G.; Mears, C.; Po-Chedley, S.; Fu, Q.; Wentz, F.; Zou, C.; Painter, J.; Cvijanovic, I. Comparing Tropospheric Warming in Climate Models and Satellite 24 Data. *J. Clim.* **2017**, *30*, 373–392. [CrossRef]
48. Santer, B.D.; Solomon, S.; Wentz, F.J.; Fu, Q.; Po-Chedley, S.; Mears, C.; Painter, J.F.; Bonfils, C. Tropospheric warming over the past two decades. *Sci. Rep.* **2017**, *7*, 2336. [CrossRef]
49. Santer, B.D.; Painter, J.F.; Bonfils, C.; Mears, C.A.; Solomon, S.; Wigley, T.M.L.; Gleckler, P.J.; Schmidt, G.A.; Doutriaux, C.; Gillett, N.P.; et al. Human and natural influences on the changing thermal structure of the atmosphere. *Proc. Natl. Acad. Sci. USA* **2013**, *110*, 17235–17240. [CrossRef]
50. IPCC. *Climate Change 2013: The Physical Science Basis. Contribution of Working Group I to the Fifth Assessment Report of the Intergovernmental Panel on Climate Change*; Stocker, T.F., Qin, D., Plattner, G.-K., Tignor, M., Allen, S.K., Boschung, J., Nauels, A., Xia, Y., Bex, V., Midgley, P.M., Eds.; Cambridge University Press: Cambridge, UK; New York, NY, USA, 2013.
51. Jakovlev, A.R.; Smyshlyaev, S.P. The numerical simulations of global influence of ocean and El-Nino—La-Nina on structure and composition of atmosphere. *Uchonie Zapiski RSHU* **2017**, *49*, 58–72. (In Russian)

52. Jakovlev, A.R.; Smyshlyaev, S.P. Numerical Simulation of World Ocean Effects on Temperature and Ozone in the Lower and Middle Atmosphere. *Russ. Meteorol. Hydrol.* **2019**, *44*, 594–602. [CrossRef]
53. Jakovlev, A.R.; Smyshlyaev, S.P. Impact of the Southern Oscillation on Arctic Stratospheric Dynamics and Ozone Layer. *Izv. Atmos. Ocean. Phys.* **2019**, *55*, 86–99. [CrossRef]
54. Jakovlev, A.R.; Smyshlyaev, S.P. Simulation of influence of ocean and El-Nino—Southern oscillation phenomenon on the structure and composition of the atmosphere. In Proceedings of the IOP Conference Series: Earth and Environmental Science (EES), CITES-2019, Moscow, Russia, 13–14 November 2019.
55. Gelaro, R.; McCarty, W.; Suárez, M.J.; Todling, R.; Molod, A.; Takacs, L.; Randles, C.; Darmenov, A.; Bosilovich, M.; Reichle, R.; et al. The Modern-Era Retrospective Analysis for Research and Applications, Version 2 (MERRA-2). *J. Clim.* **2017**, *30*, 5419–5454. [CrossRef] [PubMed]
56. Hoffmann, L.; Günther, G.; Li, D.; Stein, O.; Wu, X.; Griessbach, S.; Heng, Y.; Konopka, P.; Müller, R.; Vogel, B.; et al. From ERA-Interim to ERA5: The considerable impact of ECMWF's next-generation reanalysis on Lagrangian transport simulations. *Atmos. Chem. Phys.* **2019**, *19*, 3097–3124. [CrossRef]
57. Weather and Climate Change/Met Office. Available online: http://https://www.metoffice.gov.uk/hadobs/hadgem_sst/data/download.html (accessed on 20 March 2021).
58. Galin, V.Y.; Smyshlyaev, S.P.; Volodin, E.M. Combined Chemistry–Climate Model of the Atmosphere. *Izv. Atmos. Ocean. Phys.* **2007**, *43*, 399–412. [CrossRef]
59. Sunspot Index and Long-Term Solar Observations (SILSO) Data/Image. Royal Observatory of Belgium: Belgium, Brussels. Available online: http://www.sidc.be/silso/home (accessed on 15 December 2020).
60. Smyshlyaev, S.P.; Geller, M.A. Analysis of SAGE II observations using data assimilation by the SUNY-SPB two-dimensional model and comparison to TOMS data. *J. Geophys. Res.* **2001**, *106*, 32327–32335. [CrossRef]
61. Wang, S.; Liu, C.-L.; Zheng, L. Feature Selection by Combining Fisher Criterion and Principal Feature Analysis. In Proceedings of the Sixth International Conference on Machine Learning and Cybernetics, Hong Kong, China, 19–22 August 2007; Volume 2, pp. 1149–1154.
62. Smyshlyaev, S.P.; Galin, V.Y.; Shaariibuu, G.; Motsakov, M.A. Modeling the Variability of Gas and Aerosol Components in the Stratosphere of Polar Regions. *Izv. Atmos. Ocean. Phys.* **2010**, *46*, 265–280. [CrossRef]
63. Dianskii, N.A.; Galin, V.Y.; Gusev, A.V.; Volodin, E.M.; Iakovlev, N.G.; Smyshlyaev, S.P. The model of the Earth system developed at the INM RAS. *Russ. J. Numer. Anal. Math. Model.* **2010**, *25*, 419–429. [CrossRef]
64. Smyshlyaev, S.P.; Galin, V.J.; Atlaskin, E.M.; Blakitnaya, P.A. Simulation of indirect influence of eleven cycle of solar activity on gaseous composition of atmosphere. *Izv. Atmos. Ocean. Phys.* **2010**, *46*, 672–684.
65. Thomson, A.M.; Calvin, K.V.; Smith, S.J.; Kyle, G.P.; Volke, A.; Patel, P.; Delgado-Arias, S.; Bond-Lamberty, B.; Wise, M.A.; Clarke, L.E. RCP 4.5: A pathway for stabilization of radiative forcing by 2100. *Clim. Chang.* **2011**, *109*, 77–94. [CrossRef]
66. Scientific Assessment of Ozone Depletion: 2018. World Meteorological Organization Global Ozone Research and Monitoring Project—Report No. 58. Available online: https:www.esrl.noaa.gov/csl/assessments/ozone/2018/downloads/2018OzoneAssessment.pdf (accessed on 20 March 2021).
67. Haumann, F.A.; Gruber, N.; Münnich, M. Sea-ice induced Southern Ocean subsurface warming and surface cooling in a warming climate. *AGU Adv.* **2020**, *1*, e2019AV000132. [CrossRef]
68. Cobb, K.M.; Charles, C.D.; Cheng, H.; Edwards, R.L. El Niño/Southern Oscillation and tropical Pacific climate during the last millennium. *Nat. Cell Biol.* **2003**, *424*, 271–276. [CrossRef] [PubMed]
69. Grove, R.; Adamson, G. El-Nino of world history. In *Palgrave Studies in World Environment*; Palgrave Macmillan: London, UK, 2018; 251p.
70. Smyshlyaev, S.P.; Galin, V.Y.; Blakitnaya, P.A.; Jakovlev, A.R. Numerical Modeling of the Natural and Manmade Factors Influencing Past and Current Changes in Polar, Mid-Latitude and Tropical Ozone. *Atmosphere* **2020**, *11*, 76. [CrossRef]